AD-A034 726

EVALUATION OF PROBE SAMPLING VERSUS OPTICAL IN
SITU MEASUREMENTS OF NITRIC OXIDE CONCENTRATIONS
IN A JET ENGINE COMBUSTOR EXHAUST

ARNOLD ENGINEERING DEVELOPMENT CENTER
ARNOLD AIR FORCE STATION, TENNESSEE

JANUARY 1977

EVALUATION OF PROBE SAMPLING VERSUS OPTICAL IN SITU

MEASUREMENTS OF NITRIC OXIDE CONCENTRATIONS

IN A JET ENGINE COMBUSTOR EXHAUST

ENGINE TEST FACILITY
ARNOLD ENGINEERING DEVELOPMENT CENTER
AIR FORCE SYSTEMS COMMAND
ARNOLD AIR FORCE STATION, TENNESSEE 37389

January 1977

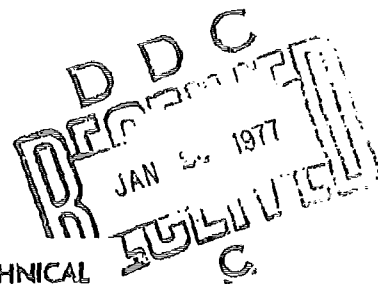Final Report for Period 2 July 1974 — 16 February 1975

Prepared for

DEPARTMENT OF TRANSPORTATION
CAMBRIDGE, MASSACHUSETTS 02142

and

DIRECTORATE OF TECHNOLOGY
ARNOLD ENGINEERING DEVELOPMENT CENTER
ARNOLD AIR FORCE STATION, TENNESSEE 37389

45

This report has been reviewed by the Information Office (OI) and is releasable to the National Technical Information Service (NTIS). At NTIS, it will be available to the general public, including foreign nations.

APPROVAL STATEMENT

This technical report has been reviewed and is approved for publication.

FOR THE COMMANDER

EULES L. HIVELY
Research and Development
   Division
Directorate of Technology

ROBERT O. DIETZ
Director of Technology

i

REPORT DOCUMENTATION PAGE		READ INSTRUCTIONS BEFORE COMPLETING FORM
1 REPORT NUMBER AEDC-TR-76-180	2 GOVT ACCESSION NO	3 RECIPIENT'S CATALOG NUMBER
4 TITLE (and Subtitle) EVALUATION OF PROBE SAMPLING VERSUS OPTICAL IN SITU MEASUREMENTS OF NITRIC OXIDE CONCENTRATIONS IN A JET ENGINE COMBUSTOR EXHAUST		5 TYPE OF REPORT & PERIOD COVERED Final Report, 2 July 1974 - 16 February 1975
		6 PERFORMING ORG. REPORT NUMBER
7 AUTHOR(s) J. D. Few, R. J. Bryson, and W. K. McGregor, ARO, Inc.		8 CONTRACT OR GRANT NUMBER(s)
9 PERFORMING ORGANIZATION NAME AND ADDRESS Arnold Engineering Development Center (DY) Air Force Systems Command Arnold Air Force Station, TN 37389		10 PROGRAM ELEMENT, PROJECT, TASK AREA & WORK UNIT NUMBERS Program Element 65807F
11 CONTROLLING OFFICE NAME AND ADDRESS Arnold Engineering Development Center (DYFS), Arnold Air Force Station, TN 37389		12 REPORT DATE January 1977
		13 NUMBER OF PAGES 42
14 MONITORING AGENCY NAME & ADDRESS(If different from Controlling Office)		15. SECURITY CLASS. (of this report) UNCLASSIFIED
		15a DECLASSIFICATION/DOWNGRADING SCHEDULE N/A

16 DISTRIBUTION STATEMENT (of this Report)

Approved for public release; distribution unlimited.

17 DISTRIBUTION STATEMENT (of the abstract entered in Block 20, if different from Report)

18 SUPPLEMENTARY NOTES

Available in DDC.

19 KEY WORDS (Continue on reverse side if necessary and identify by block number)

emission
engines
exhaust gases
probes
samplers
absorption (physical)
optics

20 ABSTRACT (Continue on reverse side if necessary and identify by block number)

Measurements of nitric oxide (NO) concentrations were made at the exhaust of a jet engine combustor by conventional gas-sampling probe and chemiluminescent analyzer methods, by optical resonance absorption through absorption cells located within the gas sample transfer line, and by optical resonance absorption directly through the combustor exhaust. The combustor was exhausted to atmospheric pressure and was operated at an inlet temperature near 600°F, a

DD FORM 1473 EDITION OF 1 NOV 65 IS OBSOLETE
1 JAN 73

20. ABSTRACT (Continued)

total pressure of about 3 to 4 atm, and at fuel-to-air ratios (f/a) from 0.01 to 0.05. A tubular inlet, liquid-cooled, stainless steel sampling probe was inserted into the gas stream at the combustor exit. The optical technique used was the resonance absorption method for the (0,0) γ-band of NO at wavelengths ranging from 2,200 to 2,270 Å. The results showed that within the sampling line both the chemiluminescent gas analyzer and the optical absorption method gave NO concentrations that agreed within about 20 percent (from approximately 50 ppm at f/a = 0.01, to 260 ppm at f/a = 0.05), while the direct optical absorption measurement through the combustor exhaust gave NO concentration values a factor of about 3.5 to 6 larger (from approximately 175 ppm at f/a = 0.01 to 1,600 ppm at f/a = 0.05). The impact of these findings on measurement standardization and on combustor development is discussed.

iii

PREFACE

1

CONTENTS

ILLUSTRATIONS

Figure

Preceding page blank   3

1.0 INTRODUCTION

The measurement of exhaust product species concentrations from combustion systems is usually accomplished by capturing a gas sample in the exhaust plume with a probe and analyzing the gas for the desired species, either by laboratory analysis using sample bottles or by use of online analyzers. Concern for pollutant emission species from aircraft jet engines prompted a committee of the Society of Automotive Engineers (SAE) to propose standards for the probing and measurement instruments. These standards were subsequently adopted by the Environmental Protective Agency (EPA) to be used throughout industry and the Department of Defense (Ref. 1). The Arnold Engineering Development Center (AEDC) is engaged in all phases of jet engine testing and has met the needs of several test programs by providing emissions measurement systems based on the specifications of Ref. 1. Measurement results using these systems are reported in Refs. 2, 3, 4, and 5.

During the course of one of the referenced test programs (Ref. 4), it was requested that measurements of the concentration of the OH radical be obtained in the exhaust of a YJ93-GE-3 engine which was being tested under simulated high altitude conditions in ETF Test Cell J-2. The method to be used for the OH concentration measurements was the in situ resonance line absorption technique developed previously at AEDC (Ref. 6). The in situ technique was required because of the short-lived nature of the OH radical, which does not survive in the sample tube. The resonance line absorption method has also been developed for the nitric oxide (NO) molecule (Ref. 7) and during a few of the test runs was used to determine NO concentration. The results of these measurements are reported in Refs. 4 and 8. The OH concentration measurements could not be compared with other methods, but the NO concentration obtained by the in situ method was much greater (factors of 2 to 5) than the concentration simultaneously measured in the gas sampling line by the EPA-approved analyzer instruments. This result prompted an evaluation program conducted at AEDC, which is reported here.

The in situ versus probe-sampling evaluation program required (1) the development of a source of combustion gas having species concentration values comparable to those of jet engine exhausts, (2) measurements of pollutant species concentration by in situ and probe gas-sampling methods at the same combustion gas condition, and (3) measurements of species concentration in the gas sample lines by alternate methods other than the approved analysis instruments. The combustor gas source was obtained by use of a turbine engine combustor (5.5 in.-diam AVCO-Lycoming development model loaned to AEDC) and associated heated air supply and fuel system in the R-2C Propulsion Research Area of the Engine Test Facility (ETF). The emissions analyzer package used in previous programs (Refs. 4 and 5) was adapted for use in the R-2C installation, a probe of

configuration almost identical to that used in Ref. 4 was constructed, and a heated sample gas transfer line was designed and fabricated which contained optical absorption cells near the probe and near the analyzer package. The absorption cells located within the gas sample transfer lines provide for comparison between the optical and gas analyzer measurements and account for any changes in NO concentration along the sample gas transfer line. Resonance absorption systems for measurement of NO concentration identical to the one used in the engine measurements (Ref. 8) were adapted for measurements of absorption directly through the gas stream and through the absorption cells in the transfer lines. The program for evaluation of measurement of NO concentration by the two techniques, gas sampling and resonance absorption, has been completed, and the results are reported herein.

2.0 DESCRIPTION OF APPARATUS

The experimental apparatus described in this report was installed in the Combustor Research Test Area (designated R-2C) of the Engine Test Facility. The apparatus was designed to facilitate the measurement of turbine engine combustor exhaust species concentrations by two independent measurement techniques. The test installation included a turbine engine combustor and associated operational equipment, the test section, two resonance spectral absorption systems, and a conventional gas analysis system with a stainless steel, constant area gas sample probe and a stainless steel transfer line. Optical absorption cells were placed in the transfer line at locations just downstream of the probe and just upstream of the analyzer system, to permit optical measurements of species concentrations within the sampling line. The layout of this apparatus is shown in Fig. 1.

2.1 COMBUSTOR SYSTEM AND TEST SECTION

The plenum, which enclosed the combustor (Fig. 1), was connected to the high pressure air supply by a 3-in.-diam insulated pipe which contains a control valve upstream of a calibrated critical venturi (0.95-in. diam), enabling the desired mass flow to be measured and controlled. Downstream of the calibrated venturi a propane-fired heat exchanger heated the inlet air to the desired temperature. The heater is capable of heating 5 lbm/sec of nonvitiated air up to $1,000°F$ at a pressure up to 120 psia. The insulated air supply line was connected to a 16-in.-diam plenum section in which an AVCO-Lycoming cylindrical (5.5-in. diam) combustor was housed (Fig. 2). The combustor exhausted into the test section through a standard ASME long radius convergent nozzle having an exit diameter of 2.16 in. A pressure-controlled tank supplied JP4 fuel to the combustor as shown in Fig. 3, and the flow was measured by two turbine flowmeters.
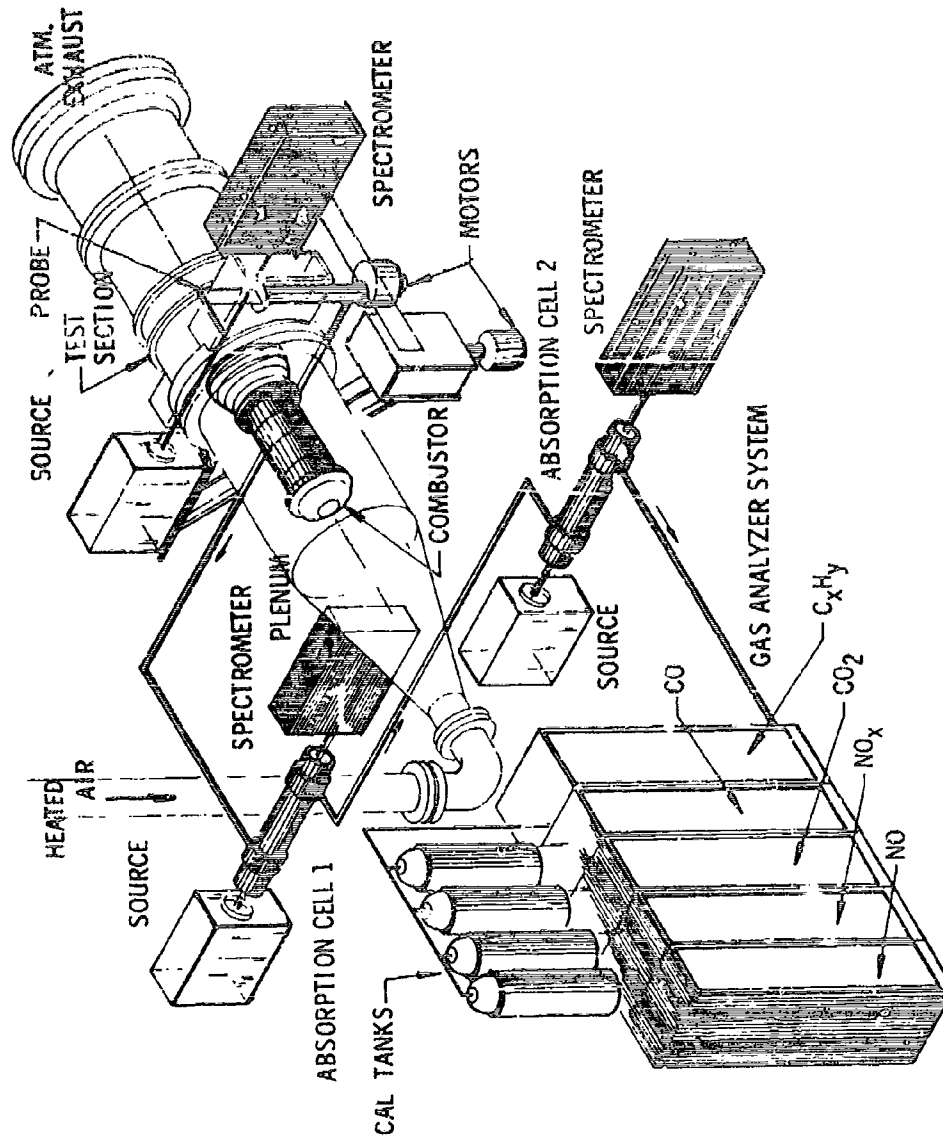
Figure 1. Sketch of experimental apparatus used for evaluation of exhaust emissions measurements methods.

7
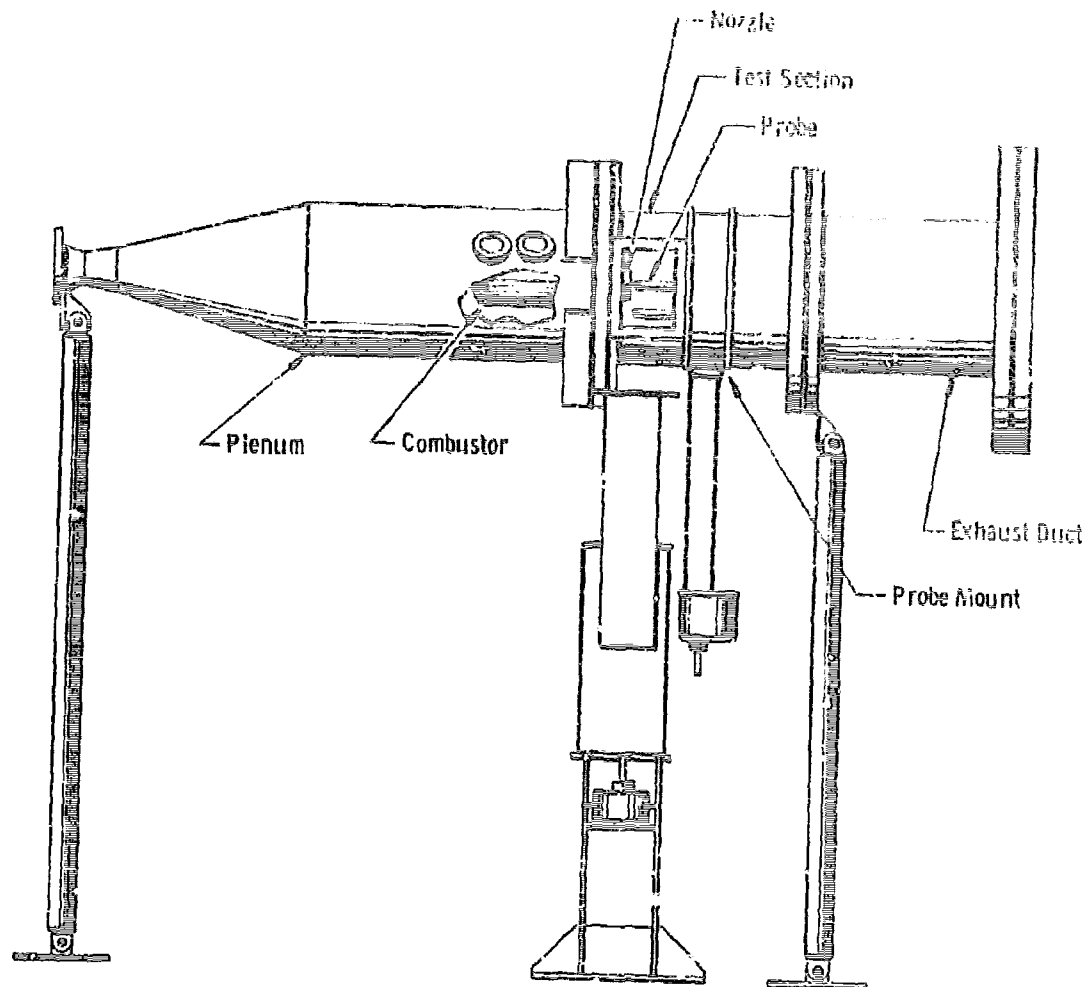
Figure 2. Sketch of a combustor installation in R-2C-1.

Pressure Controller

N₂

150-gal Fuel Tank

Fuel

Turbine Flowmeters

Secondary Air Flow

Cooling Water

To Atmosphere

Combustor

PT TC

PT TC

ASME Long Radius Nozzle, 2.16-in. Diam

Heater

Propane

PT TC

Venturi

PT TC

Control Valve

Air Supply, 4,000 psi
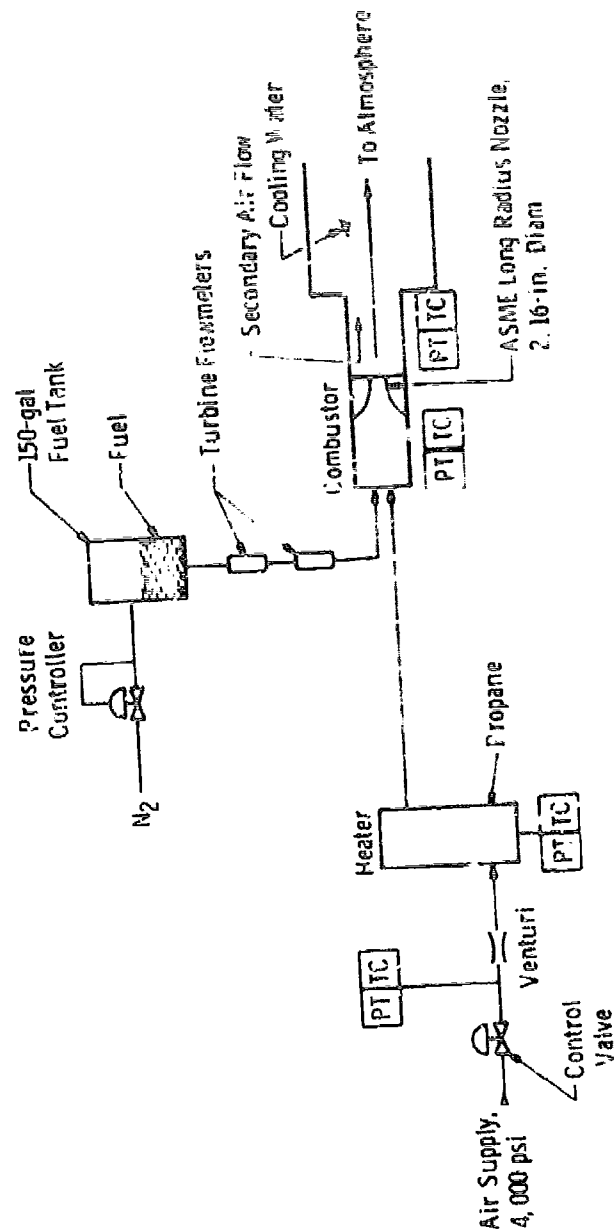
Notes:

1. Weight Flow Measurement
   Calibrated Venturi - 5 lb/sec (max)

2. Propane Heater
   Pressure Limit - 120 psia
   Temperature - 1,000°F (max)

3. PT Pressure Transducer
   TC Thermocouple

Figure 3. Diagram of the R-2C-1 air supply and fuel supply system.

9

Test cell and combustor monitoring and operating instrumentation consisted of conventional pressure transducers, gages, and thermocouples. The operation was performed in a control room located adjacent to the test area. The critical operating variables (plenum pressure, air supply temperature, etc.) and monitoring parameters (wall temperatures, etc.) were recorded by an online digital data acquisition system and displayed in the control room on a cathode ray tube (CRT). Airflow rate, fuel to air weight flow ratio, and combustor temperature were computed on line from measured variables and were also displayed on the CRT. Estimates of the uncertainty in the combustor operating parameters are given in Table 1, where the uncertainty values were determined from uncertainty values of the measured variables using methods outlined in Ref. 9.

Table 1. Estimates of Uncertainty for Combustor Operating Parameters

Parameter	Units	Nominal	Precision, percent	Bias, percent	Uncertainty, percent
Air Mass Flow Rate ($\dot{m}_a$)	lb/sec	2.5	±0.14	±0.46	±0.75
Fuel Mass Flow Rate ($\dot{m}_f$)	lb/sec	0.05	±0.75	±2.0	±3.5
Fuel to Air Ratio (f/a)	---	0.02	±0.8	±2.1	±3.7
Plenum Pressure (P_0)	psia	50	±0.1	±0.3	±0.5
Test Section Pressure (P_c)	psia	13	±0.1	±0.3	±0.5

The test section included a controlled secondary airflow system, consisting of a manifold containing a series of 0.5-in.-diam holes placed cylindrically about the nozzle exit (on a 14-in.-diam circle) to control and prevent recirculation of the exhaust gas into the region of the test section where the optical measurements were to be made. The total mass flow was exhausted to atmosphere through water cooling sprays. The test section contained optical viewing ports located on either side of the test section and centered 0.5 in. downstream of the nozzle exit. The test section operated at pressures slightly less than atmospheric, and the windows were Plexiglas® in which slots (1/4 in. wide by 4 in. high) to accommodate the optical beams had been milled (Figs. 3 and 4).
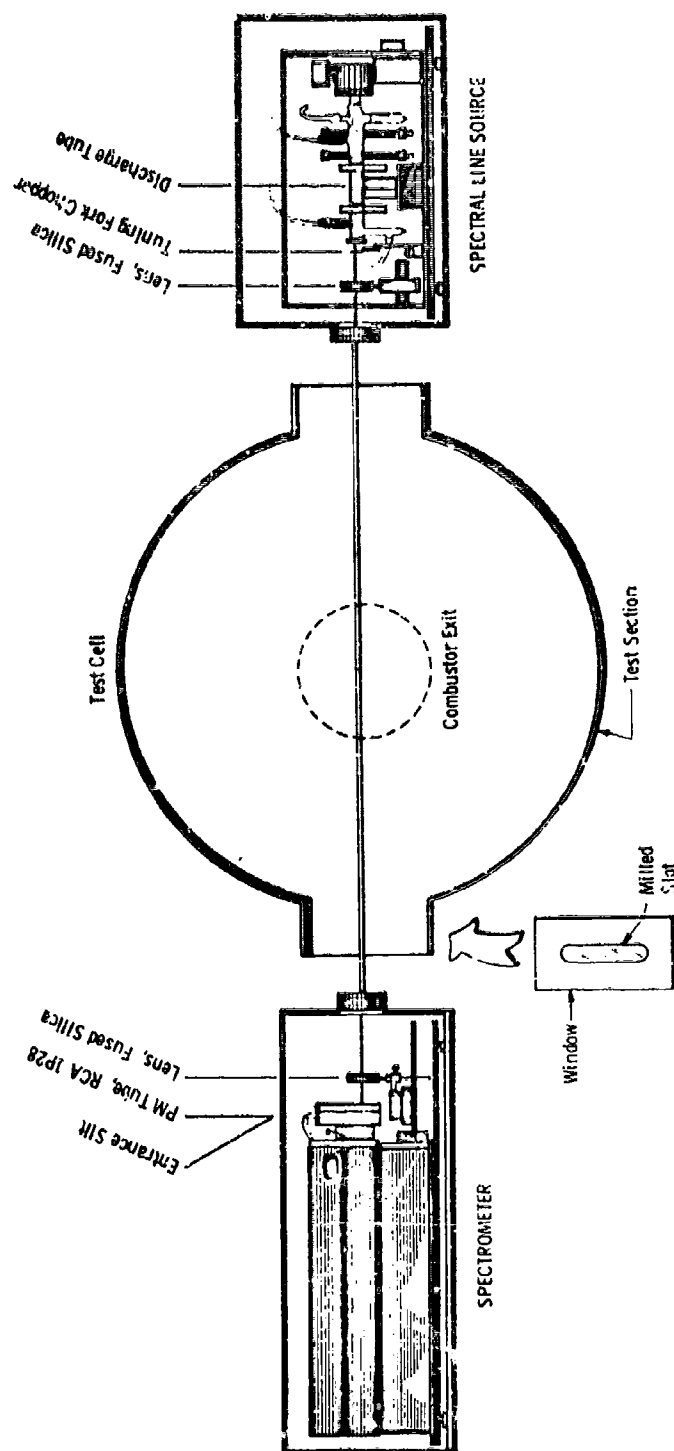
Figure 4. Illustration of physical arrangement for the in situ resonance
line absorption measurements.

Mounted below the test section, as shown in Figs. 1 and 3, was a movable yoke with mounting plates approximately 20 in. apart, which could be positioned at any height, or traversed continuously across the test section. The in situ optical measurement devices (consisting of a source and receiver) were mounted on the yoke and aligned to view a small path (0.25-in. diam) through the exhaust plume (Fig. 4). The spectral measurement could be made on plume centerline, or a traverse could be made of the plume at fixed wavelength. The sample probe was located in the test section so that the probe entrance plane coincided with that of the optical path. The probe could also be traversed across the plume radius or positioned at any desired radial position in the plume.

2.2 RESONANCE ABSORPTION SYSTEM

The in situ resonance absorption system, located as shown in Fig. 4, consisted of a spectral line source with transmitting optics and a 0.5-m spectrometer with receiving optics located on opposite sides of the test section. The source was a high voltage (3,000-v DC) capillary discharge tube through which a 12:3:1 mixture (by volume) of argon, nitrogen, and oxygen (A, N_2, and O_2), respectively, flowed at a pressure of 6 torr. The discharge tube was water cooled to provide a low temperature of the gas mixture, thus ensuring a narrow line source. The source radiation characteristics will be described in Appendix A of this report. The spectrometer (receiver) used in this experiment was a 0.5-m, Czerny-Turner type mount, grating instrument with a 2,360 groove/mm grating blazed for maximum reflection at 3,000 Å. The spectrometer was equipped with curved slits which were opened to 200μ. The 200-μ slit width resulted in a 1.6-Å bandpass for the instrument. An RCA 1P28 photomultiplier tube was used as a detector. The signal-conditioning and data-recording system is shown in Fig. 5.

The resonance absorption system used for measurements in the gas sample line was identical to the one described for the in situ measurements in the exhaust stream, except that the spectrometer used a 1,180-groove/mm grating in second order and a 200-μ slit width, again giving a bandpass of 1.6 Å. Two locations were available to make absorption measurements in the sample gas transfer line. The first location was near the probe exit ($\approx$ 4 ft from probe tip), and the second ($\approx$ 40 ft downstream) was near the entrance to the gas analysis system. The absorption measurements were made simultaneously with the NO chemiluminescent analyzer measurements. The absorption cells located in the transfer line (see Fig. 1) were 62.5-cm-long, 5-cm-diam stainless steel tubes with fused silica windows. The tubes were heated with electrical heating tape, and the temperature was controlled to the same temperature as the transfer lines (300°F). A pressure transducer was installed on both absorption cells so that a continuous pressure readout was recorded for each run condition.
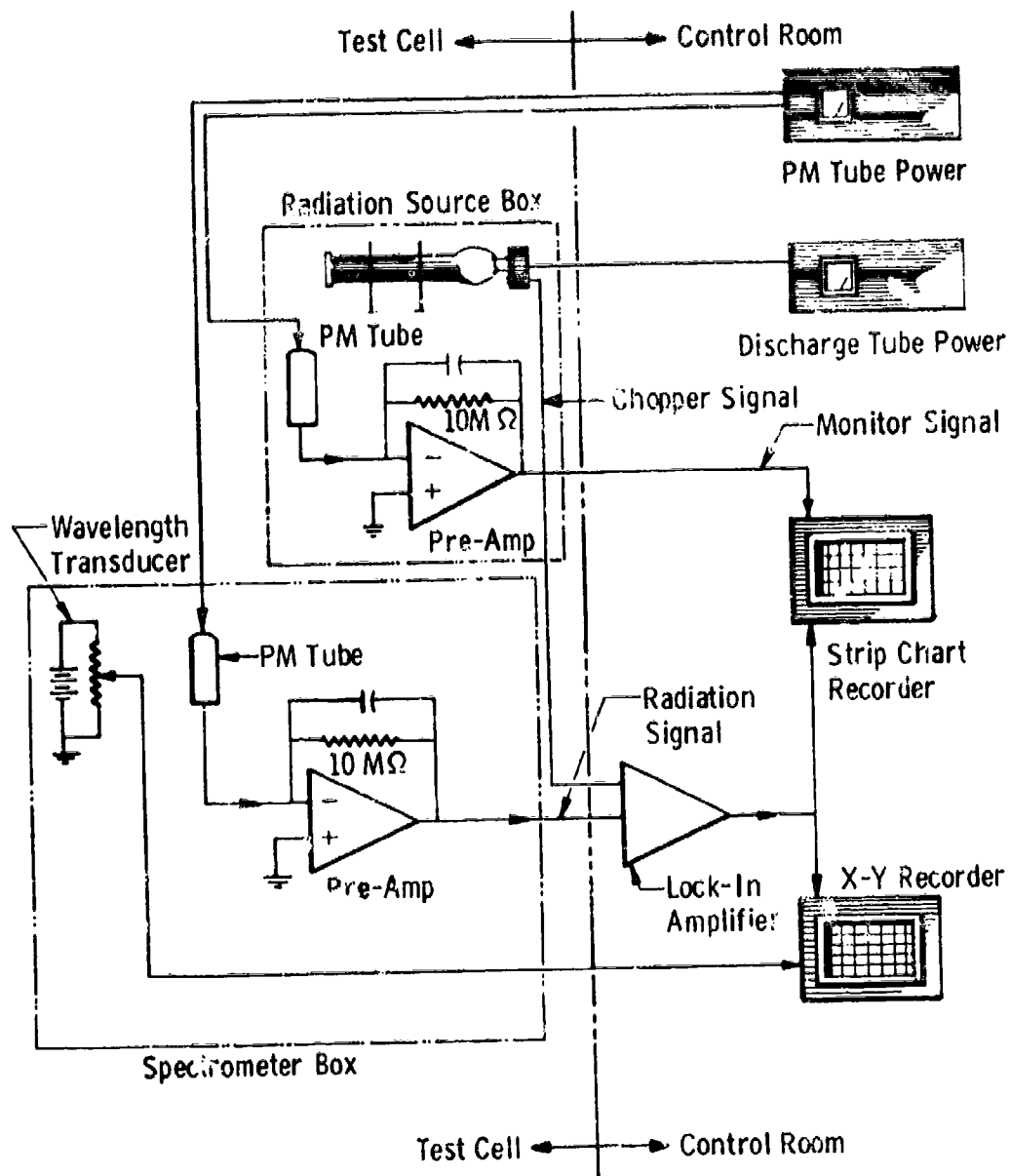
Figure 5. Electrical schematic of spectral absorption system.

2.3 GAS ANALYSIS SYSTEM

The Society of Automotive Engineers E-31 committee has established guidelines for the design of sample systems and testing approaches to be used in the acquisition of emissions data on turbine engines. These guidelines are contained in Aerospace Recommended Practice (ARP) Number 1256 (Ref. 1). Although this standard does not address the problems encountered in acquisition of data behind afterburning engines, it was adhered to in the design of the AEDC emissions measurement system (Ref. 4). A flow diagram of the analysis system is shown in Fig. 6. The gas sample passes through the
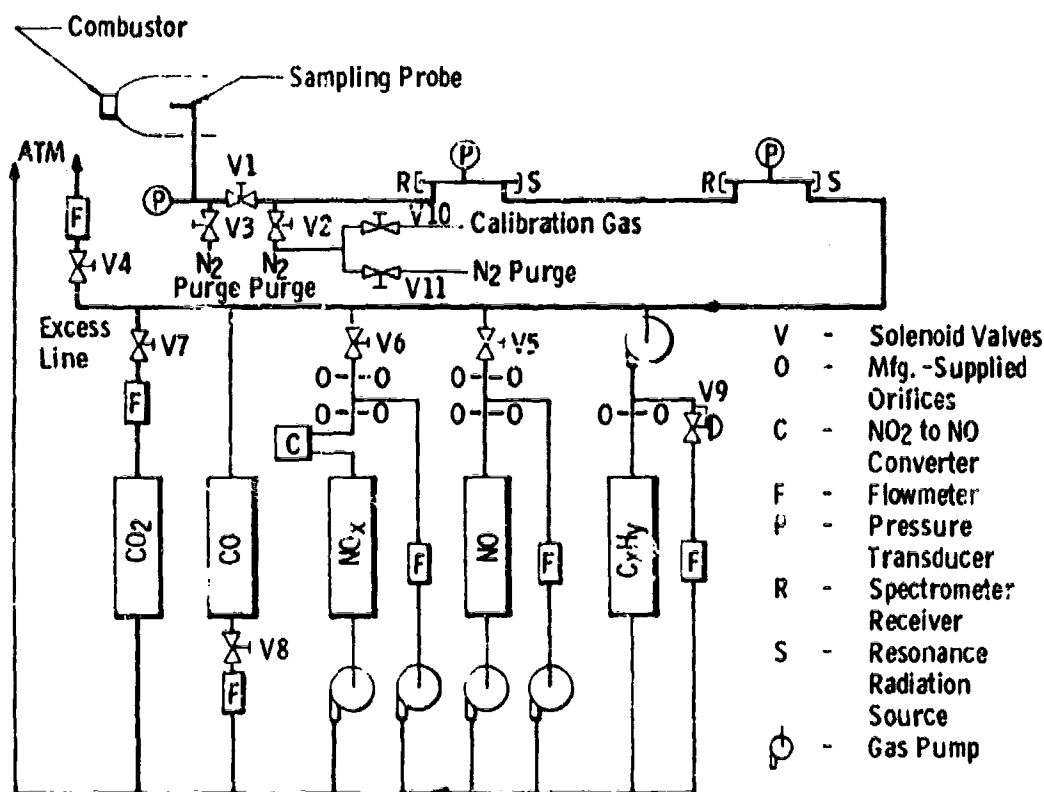
Figure 6. Diagram of probe sampling, transfer line, and emissions analyzer system.

heated transfer line, which is maintained at 300 ±10°F, through the two heated optical absorption cells, and into the five analysis instruments. The flow rate through each instrument and the flow rate through the excess line were measured using volume flow, ball-type flowmeters. The analysis panel used in this study contained five types of instruments (Fig. 7). The types and models of these instruments were as follows:

1. NO: chemiluminescence type, TECO (Model 10A, quoted accuracy = ±1 percent)

2. NO_x: chemiluminescence type, TECO (Model 10A with converter, quoted accuracy = ±1 percent)

3. CO: nondispersive infrared type, Beckman (Model 315A, quoted accuracy = ±1 percent)

4. CO_2: nondispersive infrared type, Beckman (Model 315A, quoted accuracy = ±1 percent)

5. $C_x H_y$: flame ionization detector type, Beckman (Model 402)
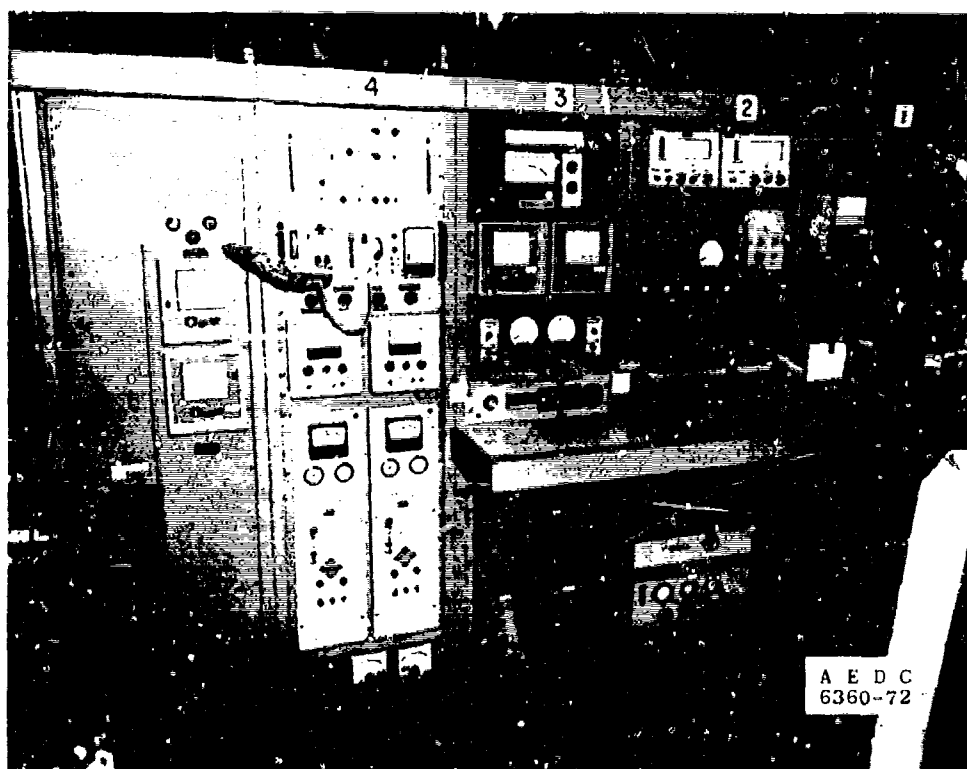
Figure 7. Photograph of gas analyzer panel.

The analyzer instruments were calibrated in place using certified calibration gases supplied by the Scott Research Corporation. A gas to establish an instrument zero and a minimum of two different calibration gases were used in the calibrations. The accuracy of

15

the concentration of the calibration gas was estimated to be ±4 percent (Ref. 10). Temperature conditioning was provided within the analyzer by steam-jacketed lines designed according to the ARP-1256 standards (Ref. 1). Standard pressure and temperature instrumentation were used to insure operation of both the analyzer and the entire emission measurement system in accordance with manufacturer's instructions.

The probe used in these studies was a straight section of 3/8-in. stainless steel tubing enclosed within a liquid-cooled housing (Fig. 8). The coolant was supplied by a high pressure pump (180 psia) from a reservoir containing a mixture of water and ethylene-glycol. The temperature of the mixture could be controlled by a series of electrical heaters located within the reservoir.
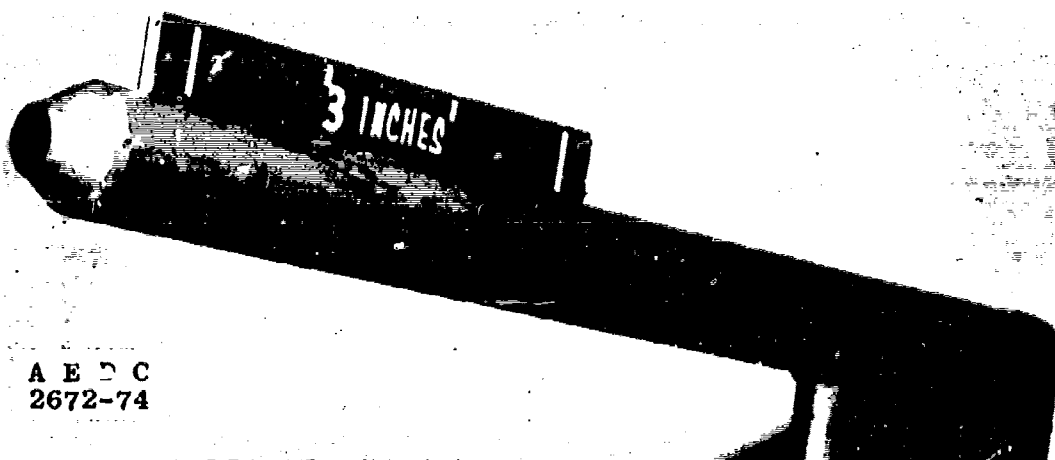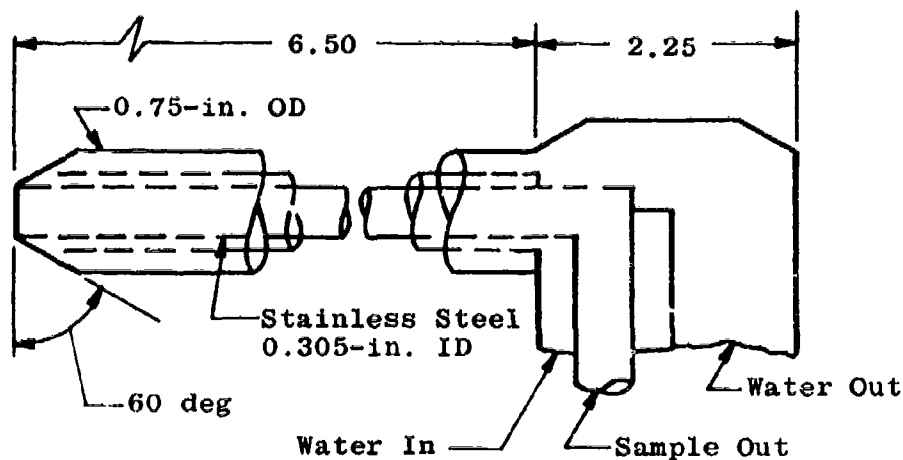
Figure 8. Photograph and sketch of tubular inlet sampling probe.

Difficulty was encountered early in this study with formation of condensate in the analyzer instruments and on the windows of the absorption cells. This problem was corrected by continually purging the lines in both directions from the sampling valve (V1 in Fig. 6) with dry nitrogen except when a measurement was being made.

3.0 RESONANCE ABSORPTION METHOD

3.1 INTRODUCTION

The use of absorption spectroscopy for species density measurements may take on many forms, depending upon the application and the molecule involved. The method employed in this work is the resonance absorption method. In this method a spectral line source is employed in which the spectral lines produced by the source have the same wavelength as the resonance lines or bands of the absorbing species. This absorption method is most useful for atoms or molecules which have an electronic resonance transition in an experimentally accessible wavelength region. Several diatomic, heteronuclear molecules which occur in combustion exhaust products (OH, NO, CH, for example) have resonance transitions in spectral regions which are accessible with conventional spectrometric apparatus. The method will be applied here to the NO molecule, which has an electronic resonance transition in the ultraviolet (≈ 2260 Å) spectral region.

Practical use of resonance absorption to make species concentration measurements requires either a comprehensive calibration over the range of concentration, pressure, and temperature to be expected during the application, or an adequate mathematical model of the radiative transfer and instrument function which can be used to make accurate predictions of the measured transmission through media as a function of concentration, pressure, and temperature. The latter approach is to be preferred for reasons of economy, but the model must be substantiated through laboratory testing. A model has been developed at AEDC which is described and verified in Refs. 11 and 12. The model consists of two parts. First, equations are developed which relate the transmission of overlapping, Doppler-broadened spectral lines in vibrational-rotational bands (the γ-bands of NO, to be specific) produced in a source lamp through absorbing gas media with combined Doppler and collision broadening. Second, a mathematical representation is made of the dispersive instrument which has a limited bandpass containing many spectral lines.

A complete treatment of the theory necessary for determining the integrated transmission of the source radiation through a medium containing molecular species which have absorption coefficient values in the frequency interval of the emission lines is given in Refs. 11 and 12. For completeness, a synopsis of the theory and presentation of the equations necessary for determining the concentration will be given in this section.

17

3.2 TRANSMISSION EQUATIONS FOR A COLLISION-BROADENED VIBRATION-ROTATION BAND

The transmissivity, t, of a beam of light of intensity $I^0_{\nu_j}$ and consisting of many spectral lines, j, through a homogeneous medium of length ℓ having absorption coefficients, k_i, which affect the transmission of $I^0_{\nu_j}$ is given by

$$t_{\Delta\nu} = \frac{\sum_j \int_{\nu^0_j - n(\Delta_a\nu_j)_D}^{\nu^0_j + n(\Delta_a\nu_j)_D} I^0_{\nu_j} \exp\left(-\ell \sum_i k_{\nu_i}\right) d\nu}{\sum_j \int_{\nu^0_j - 2(\Delta_a\nu_j)_D}^{\nu^0_j + 2(\Delta_a\nu_j)_D} I^0_{\nu_j} d\nu} \tag{1}$$

where the terms are listed in the Nomenclature and will be further defined below. The limits of integration are chosen so that all components of overlapping lines are accounted for by choice of some n number of Doppler widths from the line center. In general the frequency distribution of the absorption coefficient, k_{ν_i}, is given by (Ref. 12)

$$k_{\nu_i} = k^0_{\nu_i} \frac{1}{\pi} \int_{-\infty}^{+\infty} \frac{a' \exp(-y^2)}{a'^2 + (\omega_i - y)^2} \tag{2}$$

where y is a dummy variable and a' is the line-broadening parameter given by

$$a' = \frac{(\Delta_a\nu_i)_L}{(\Delta_a\nu_i)_D} \sqrt{\ell n\, 2} \tag{3}$$

and ω_i is the Doppler function, given by

$$\omega_i = \frac{2(\nu_i - \nu^0_i)}{(\Delta_a\nu_i)_D} \sqrt{\ell n\, 2} \tag{4}$$

In Eq. (2), $k^0_{\nu_i}$ is the absorption coefficient at line center for Doppler conditions. In Eq. (3), $(\Delta_a\nu_i)_L$ is the Lorentz half width caused by collision broadening of the absorption line. The parameter a' cannot be specified from first principles but must be measured. It is shown in Ref. 12 that for the (0,0) γ-band of NO

$$a' = 1,200\, (\pm 200)\, \frac{p}{T_a} \tag{5}$$

where p is the static pressure of the absorbing gas in atmospheres and T_a is the static temperature in degrees Kelvin.

The factor $(\Delta_a \nu_i)_D$ is the Doppler half-width of the absorption line and is given by

$$(\Delta_a \nu_i)_D = 2\nu_i^0 \sqrt{\frac{(2\ell n\ 2)KT_a}{M_a c^2}} \qquad (6)$$

where T_a is the temperature of the absorbing medium, M_a is the mass of the absorbing molecules, K is Boltzmann's constant, and c is the speed of light.

If the radiation source is maintained at low pressure, the frequency distribution of $I_{\nu_j}^0$ can be attributed to the Doppler effect and is given by

$$I_{\nu_j}^0 = I_{\nu_j}^0 0 \exp\left\{ \left[\frac{2(\nu - \nu_j^0)}{(\Delta_s \nu_j)_D} \sqrt{\ell n\ 2} \right]^2 \right\} \qquad (7)$$

where $I_{\nu_j}^0$ is the intensity of the source line at center frequency, ν_j^0, and $(\Delta_s \nu_j)_D$ is the Doppler half-width of the emitted source spectral line. The Doppler half-width of the source line is given by

$$(\Delta_s \nu_j)_D = 2\nu_j^0 \sqrt{\frac{(2\ell n\ 2)KT_s}{M_s c^2}} \qquad (8)$$

where T_s is the temperature of the source, M_s is the mass of the emitting molecule, K is Boltzmann's constant, and c is the speed of light. The distribution of the intensities of each line, j, in the spectrum must also be known. This is a property of the source and must be determined experimentally. The characteristics of the source lamp are given in Appendix A.

The absorption coefficient of a diatomic molecule for Doppler conditions at line center frequency, $k_{\nu_i}^0$, is related to properties of the absorbing medium by

$$k_{\nu_i}^0 = \frac{2e^2 \sqrt{\pi \ell n\ 2}}{M c^2} \frac{N_{J''} f_{J'J''}}{(\Delta_a \nu_i)_D} \qquad (9)$$

where e is the charge on an electron, c is the velocity of light, m is the mass of an electron, $f_{J'J''}$ is the oscillator strength of the appropriate absorption line, $N_{J''}$ is the number density of molecules in the lower energy state of the molecule corresponding to the ith line, J'' is the rotational quantum number of the lower energy state, and J' is the rotational quantum number of the upper energy state (Ref. 12).

The number density of the lower energy state, $N_{J''}$, under equilibrium conditions is given by

$$N_{J''} = \frac{hc\, B_0(2J'' + 1)\, \exp\left[-\frac{hc}{KT_a} F(J'')\right]}{2K T_a} N_0 \qquad (10)$$

where N_0 is the number density of the molecule of interest, B_0 is the rotational constant for the ground state, h is Planck's constant, K is Boltzmann's constant, and $F(J'')$ is the rotational energy term for the lower rotational energy state.

The value for the oscillator strength, $f_{J'J''}$, is given by

$$f_{J'J''} = f_{v'v''} \frac{\nu_{J'J''}}{\nu_{v'v''}} \frac{S_{J''J'}}{2(2J'' + 1)(2S + 1)} \qquad (11)$$

where $f_{v'v''}$ is the band oscillator strength, $\nu_{J'J''}$ is the frequency of the line of interest, $\nu_{v'v''}$ is the frequency at the bandhead, $S_{J''J'}$ is the normalized Honl-London factor for the line of interest, and S is the spin quantum number (Ref. 12). Combining Eqs. (9), (10), and (11),

$$k_{\nu_i}^o = \frac{e^2 \sqrt{\pi \ell n\, 2}\; h\, B_0 \nu_{J'J''} f_{v'v''} S_{J'J''} N_0 \exp\left[-\frac{hc}{KT_a} F(J'')\right]}{2(2S + 1)mcK T_a \nu_{v'v''}(\Delta_a \nu_i)_D} \qquad (12)$$

For a particular spectral line of a given molecular species for which the various molecular parameters in Eq. (12) are known, values of k_{ν_i} can be calculated as functions of N_0 and T_a. For the (0,0) γ-band of NO, Eq. (12) becomes

$$k_{\nu_i}^o = 1.603 \times 10^{-14} \frac{S_{J'J''} N_0}{T_a^{3/2}} \exp\left[-1.4383 \frac{F(J'')}{T_a}\right] \qquad (13)$$

Now all properties in Eqs. (1) and (13) are known except the transmission, $t_{\Delta\nu}$, and the molecular density, N_0; $t_{\Delta\nu}$ can be measured so that N_0 can be determined. The work of Ref. (12) was done to verify this procedure, and the technique utilizes a computer program to relate N_0 to the measured transmission through homogeneous media for a given set of experimental conditions (T_s, T_a, p, ℓ, ν, and $\Delta\nu$).

4.0 RESULTS AND DISCUSSION

4.1 CALCULATION OF SIMULATED NO γ-BAND SPECTRA

The primary purpose in the calculation of simulated spectra of the transmission of NO γ-band radiation through an absorbing path is to extend the laboratory calibration

20

data taken at limited temperature and pressures to a wider range of values applicable directly to measurement conditions. A set of simulated spectral scan data was computed for each temperature and pressure condition encountered during the experimental program, for both the in situ measurement and the absorption cell, at the appropriate path lengths. A calibration curve was then generated for each operating condition from these data such that the NO concentration could be determined in parts per million directly from these curves.

For the absorption cells located in the gas sample transfer lines the static pressure and temperature were assumed constant throughout the optical path, and the inputs to the computer program (pressure and absorber temperature) were well defined. The computed spectra of the $(0,0)$ γ-band of NO for one condition of the absorption cell ($p = 3.01$ atm, $T = 426°K$, $\ell = 62.5$ cm) are given in Fig. 9. A corresponding calibration curve was obtained by plotting the absorptivity $(1 - t)$ at the second bandhead versus the NO concentration, as shown in Fig. 10.

For the combustion gas stream the static temperature, T_a, and static pressure, p, were not as well defined as for the absorption cells, since direct measurements were not made. Rather, a method of characteristics (MOC) computer program (Ref. 13) was used to obtain p and T_a at the point 0.5 in. downstream from the exit plane for each combustor run condition as a function of radial poition. A uniform profile of gas properties at the nozzle throat was assumed in starting the MOC computer program. In this case the measured pitot pressure profile at the combustor nozzle exit was uniform as shown by the pitot pressure profile in Fig. 11, which is typical of profiles for other conditions. The total pressure used in the MOC calculation was obtained by measurement of the plenum chamber pressure corrected by an average 3-percent pressure drop across the combustor as determined by the combustor manufacturer from more detailed measurements, and the total temperature was obtained from a chemical equilibrium calculation. The equilibrium calculation was accomplished by a computer program using the technique described in Ref. 14, and data for several typical combustor operating conditions are shown in Table 2. The calculation produces an average total temperature based on the fuel to air ratio and the heating value of the fuel at the given total pressure and inlet air temperature.

An example set of data from the MOC calculation (using the computer program described in Ref. 13) is given in Table 3 for the $f/a = 0.02$ conditions of Table 2, and values of p, T_a, and a', as determined from Eq. (5) with p and t_a from the MOC calculation, are shown plotted versus the exhaust stream radius in Fig. 12. The weighted average values of p, t_a, and a' are also indicated in Fig. 12.

21

Figure 3. Example simulated spectra of NO (0,0) γ-band transmission at specified absorption cell conditions for several values of NO concentration.

Path Conditions
Temperature Source ~ 320°K
Temperature, Absolute ~ 426°K
Pressure = 3.01 atm
Path Length = 62.5 cm
a' = 8.97

Curve No.	NO, ppmv	Density, cm⁻³	Transmis- sivity
1	100	5.19 x 10¹⁵	0.668
2	200	4.04 x 10¹⁶	0.455
3	300	1.56 x 10¹⁶	0.315
4	400	2.07 x 10¹⁶	0.220
5	500	2.59 x 10¹⁶	0.163
6	600	3.11 x 10¹⁶	0.124
7	700	3.63 x 10¹⁶	0.098

Figure 10. Calibration curve for NO concentration as a function of second bandhead transmissivity taken from the spectra of Fig. 9.
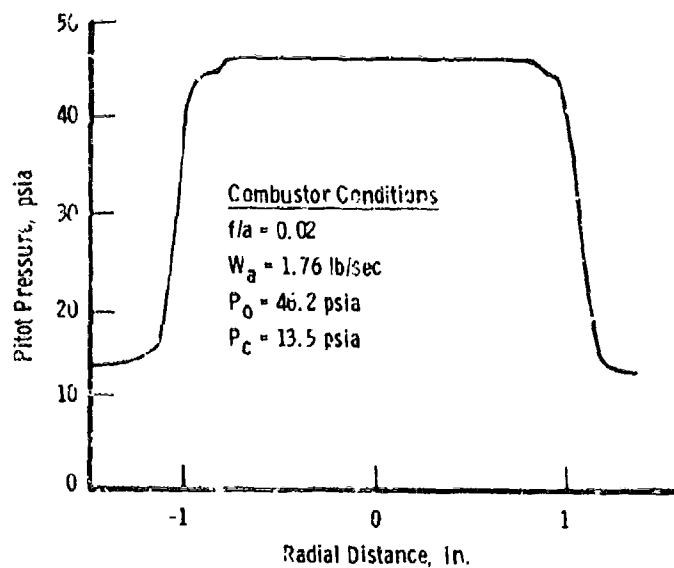
Figure 11. Pitot pressure profile 0.5 in. downstream of nozzle exit.

Table 2. Properties of Combustor Exhaust Gas for a Range of
Fuel to Air Ratios

Fuel to Air Ratio (f/a)	Inlet Air Temperature, °K	Combustor Total Pressure, psia	Test Cell Ambient Pressure, psia	*Combustor Total Temperature, °K	*Specific Heat at Constant Pressure, cal/gm, °K	*Specific Heat Ratio (Gamma)
0.01	593	55.8	13.5	1,105	0.268	1.33
0.02	566	46.2	13.5	1,340	0.282	1.31
0.03	566	50.9	13.5	1,676	0.299	1.29
0.04	572	54.8	13.5	1,935	0.310	1.28
0.05	572	56.2	13.5	2,065	0.318	1.27

*Chemical equilibrium computer program calculation, Ref. 14.

Table 3. Example Printout of Method of Characteristics Program
Used to Determine Exhaust Stream Properties

Radius, cm	Mach Number	Static Pressure, psia	Static Temperature, °K
2.96	1.47	13.6	1,001.7
2.79	1.49	13.3	996.1
2.54	1.52	12.7	986.1
2.29	1.55	12.1	973.9
2.03	1.59	11.3	959.4
1.78	1.50	12.9	990.0
1.52	1.46	13.9	1,006.1
1.27	1.41	14.8	1,022.2
1.02	1.36	15.8	1,038.3
0.76	1.32	16.8	1,054.4
0.51	1.27	17.9	1,070.0
0.25	1.23	19.1	1,085.0
0.00	1.18	20.3	1,101.7

Notes

0.5-in.-Downstream Nozzle Exit
Total Pressure = 46.2 psia
Total Temperature = 1,340 °K
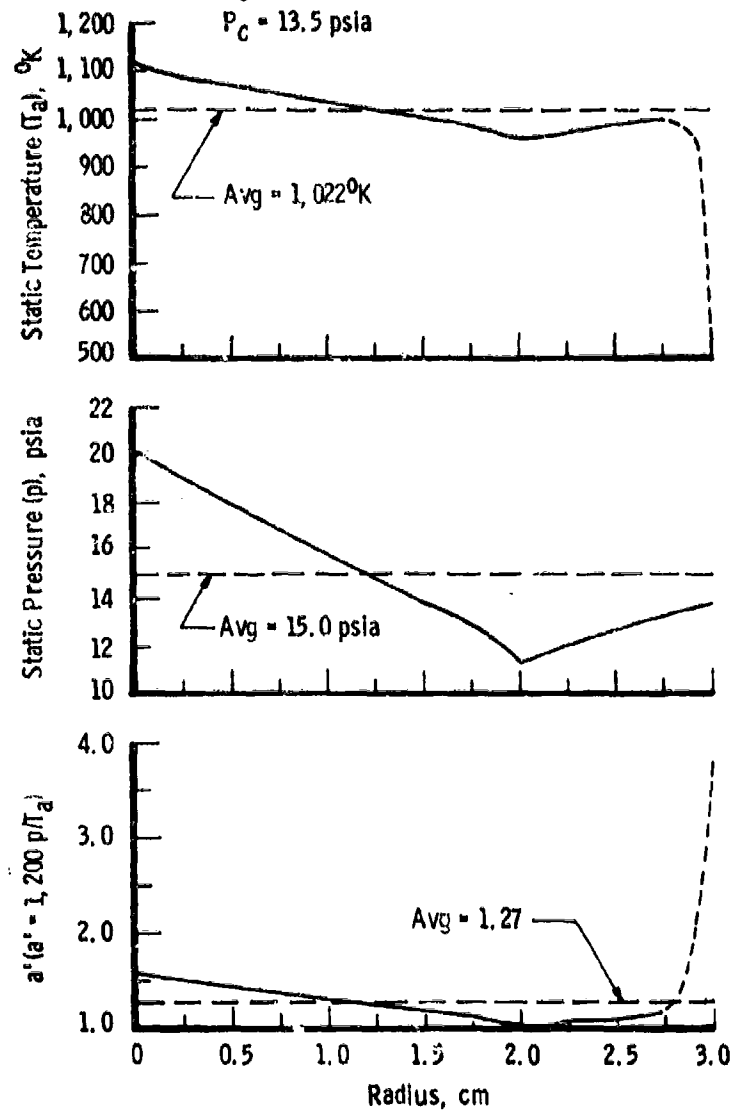
Figure 12. Temperature, pressure, and the line broadening parameter plotted as a function of radius for an example combustor condition at an axial distance 0.5 in. from the nozzle exit.

The dotted line shown at the boundary is a result of applying a turbulent mixing model (Ref. 15) to the flow process and is included to indicate a transition from the plume flow to ambient conditions. For purposes of this study this region is important only if it contributes appreciably to the optical transmission through the path. Since the static temperature is decreasing and static pressure can be assumed constant, the density increases in this mixing region. The mass fraction of plume gases, and thus the NO concentration, decrease as the radius increases. Taking the thickness, $\Delta\ell$, of the mixing layer to be 0.25 cm at the measurement station as predicted by the mixing analysis, and assuming a linear decrease in the concentration of NO, the transmission through the mixing regions on either edge of the plume is predicted to contribute less than 0.2 percent to the total transmissivity. Hence, no special consideration is given to the absorption in the mixing layer and it is included in the path length and is taken as the plume boundary as shown in Fig. 12.

In the computer-simulated calibration spectra generated for this report, the weighted average values of static temperature, static pressure, and a' taken from Fig. 12 were used. A set of calculated spectra are given in Fig. 13 for the average conditions of Fig. 12, and the corresponding calibration curve is given in Fig. 14. Note that the transmission at the second bandhead for the ranges of NO concentration given is greater than 90 percent. This condition necessitates very careful measurements of the experimental data for the in situ case.

Transmission spectra were also computed and calibration curves determined for the maximum and minimum values of static pressure and temperature and the corresponding values of a' (Fig. 12). The transmission computed at the extreme conditions of the exhaust stream pressure and temperature show negligible difference from the computed transmission from the values at the average conditions.

Because of the relatively small value of a' (a' $\approx$ 1) and the relatively large value of $(\Delta_a\nu)_D$ compared with $(\Delta_s\nu)_D$ the effect of pressure and temperature variations shown in Fig. 12 on the final value of NO concentration (Fig. 14) is small. Gradients in the NO concentration across the exhaust stream are also small, as shown by a typical radial profile of NO concentration, measured using the probe-sampling technique, in Fig. 15. This profile indicates that the NO concentration is fairly uniform across the exhaust plume and that the concentration values from the in situ measurement should not be affected appreciably by gradients in concentration or flow properties.
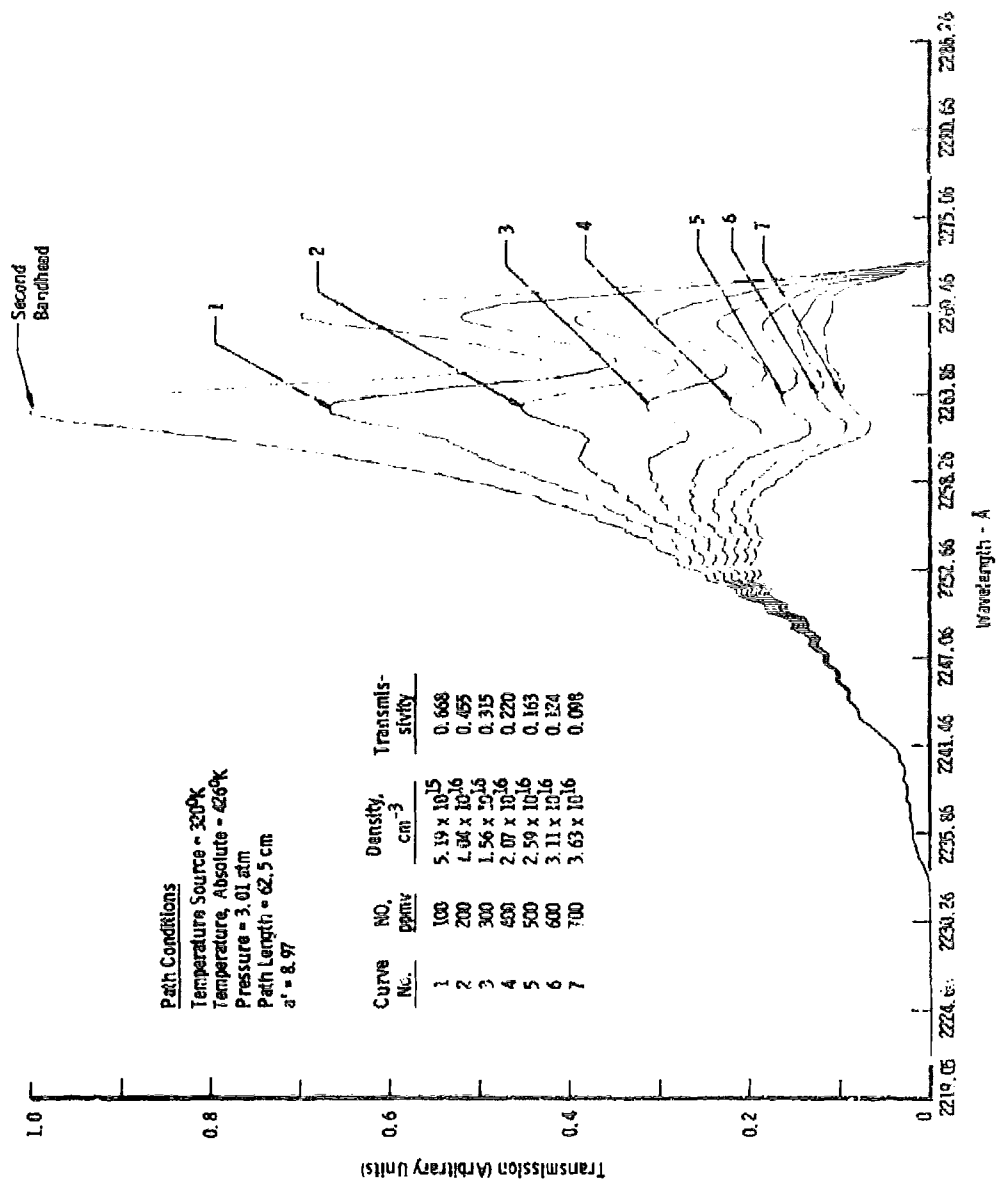
26
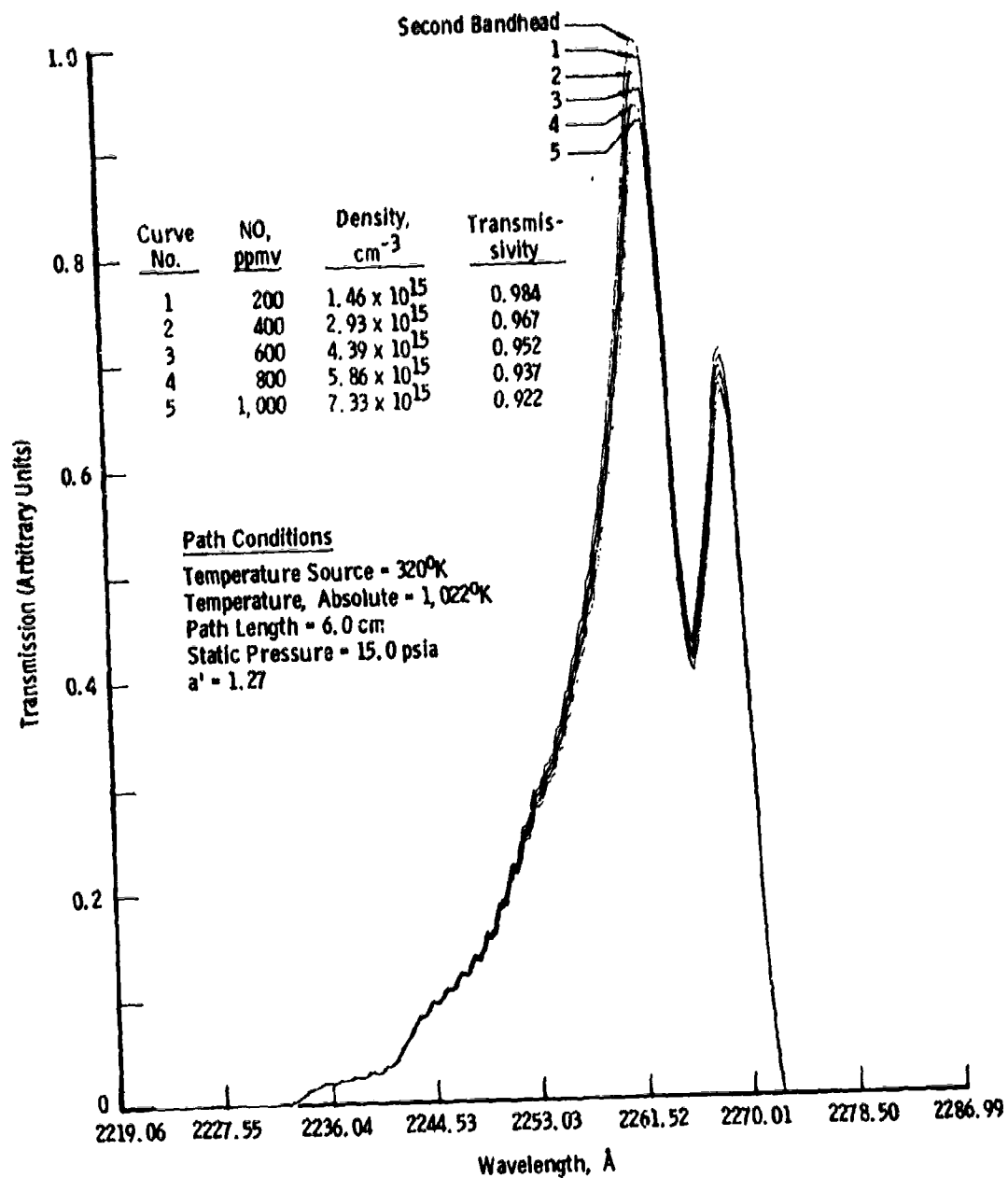
Figure 13. Example simulated spectra of NO (0,0) γ-band transmission at specified combustor conditions for several values of NO concentration.
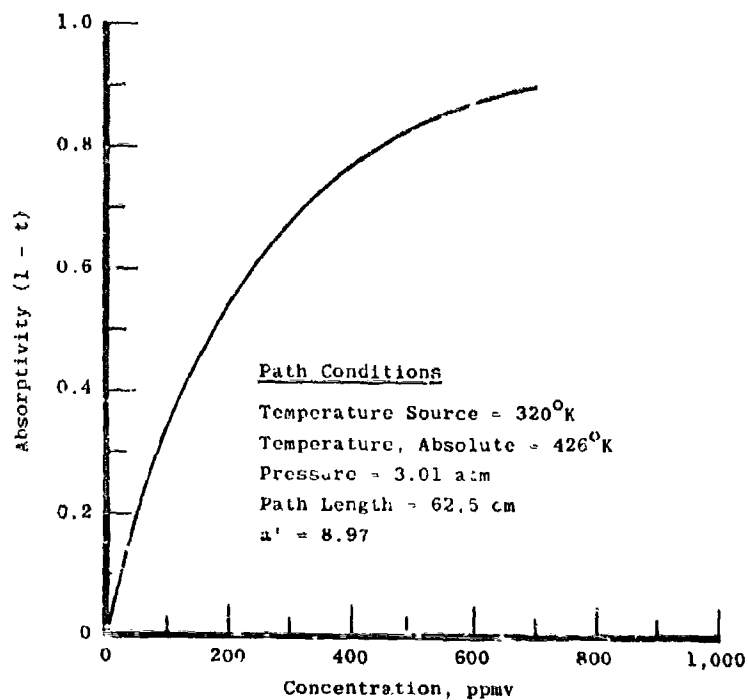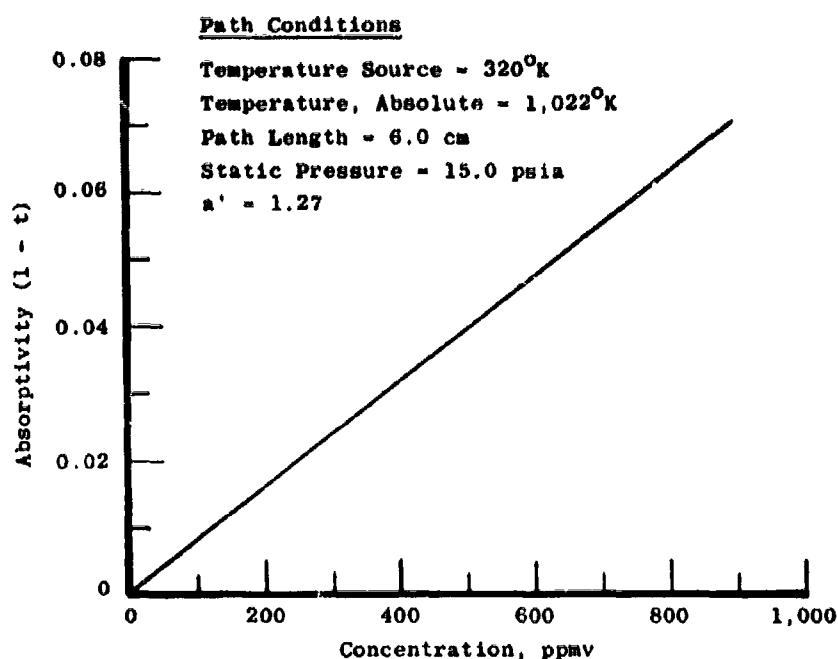
Figure 14. NO concentration as a function of transmissivity of the second band-head of the (0,0), γ-band for the average, the maximum, and the minimum possible values of the collision-broadening coefficient, a'.
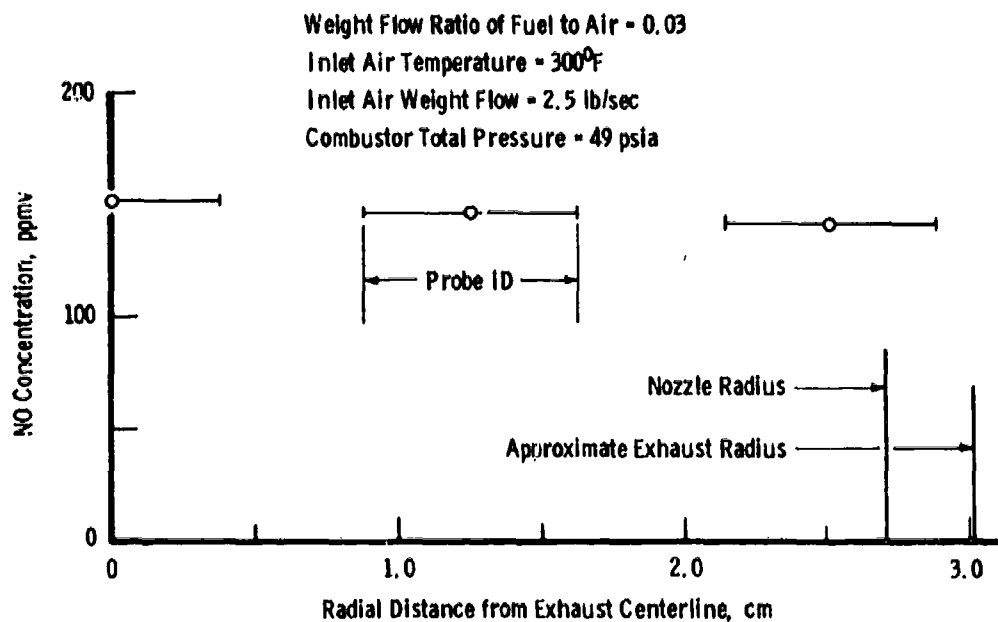
Figure 15. Typical radial profile of nitric oxide concentration as measured with the sampling probe system.

4.2 EXPERIMENTAL RESULTS

During the experiments a set of spectral scans of the NO (0,0) γ-band was obtained at both the combustor nozzle exit and in the absorption cells located in the sample gas transfer line for each combustor operating condition. The procedure was first to take NO absorption data at the combustor exit with the probe removed from the stream and with purge gas flowing through the transfer line. During this period a reference spectral trace of the transmission through the absorption cell was made. After the in situ data were obtained, the probe was inserted, the purge was turned off, emission data from the analyzer systems for all species were obtained, and transmission data through the absorption cell were taken. Example spectral scans are given for the absorption cell and for the in situ measurement in Figs. 16 and 17, respectively.

The data reduction is then straightforward and is accomplished as follows:

1. Measure the transmissivity at the peak of the second bandhead of the (0,0) γ-band from data such as Fig. 16, for the absorption tube in the sample transfer line, and Fig. 17, for the in situ measurement.

2. If necessary, correct the reference intensity at the second bandhead for drift and for extraneous absorption using the (2,2) bandhead intensity. (In Figs. 16 and 17 no correction was necessary, but this was not always the case).

3. Reading from the calibration curves of absorptivity versus concentration (Fig. 10 for the absorption cell or Fig. 14 for the in situ measurement), determine the NO concentration directly in ppmv.

The results of the emission measurements on the jet engine combustor, operated over a large range of combustor conditions, using the data reduction procedure outline above are given in Tables 4 and 5. Table 4 gives the conditions for the absorption tube and the NO concentration as determined by absorption and by the chemiluminescent analyzer. The underlined row represents the same conditions used to obtain the example calibration data, Figs. 9 and 10. Note that the absorption measurement is consistently about 20 percent larger than the chemiluminescent analyzer measurement. The data marked with an asterisk were obtained at the absorption cell nearest the analyzer instrument. No appreciable differences in the measured absorption were noted for the two locations of absorption cells. Table 5 gives the conditions used in the in situ absorption measurement through the combustor exhaust flow, and the NO concentration determined from the measurement is compared to the chemiluminescent analyzer measurement in the last two columns. The chemiluminescent analyzer data shown

represent average values since the sampling and in situ measurements were not obtained simultaneously. The underlined row represents the same conditions used to obtain the example calibration data, Figs. 12 through 14. The values of NO concentration obtained from optical measurement were much larger than those obtained from the sampling measurement.

A plot of the data given in Tables 4 and 5 is shown in Fig.18. The NO concentration determined by the in situ optical absorption method at the combustor nozzle exit, and the concentration determined by the optical absorption through the absorption cell located in the sample gas transfer line can be compared to the concentration determined by the chemiluminescence analyzer in Fig. 18. The larger differences (a factor of about 3.5 to 6) in the NO concentration obtained by in situ and gas-sampling measurement techniques is evident. The data also show that on the scale of this plot the differences between the concentration determined by the absorption measurements taken in the sample gas transfer line and the measurement made using the NO chemiluminescence gas analyzer are on the same order as the data scatter.
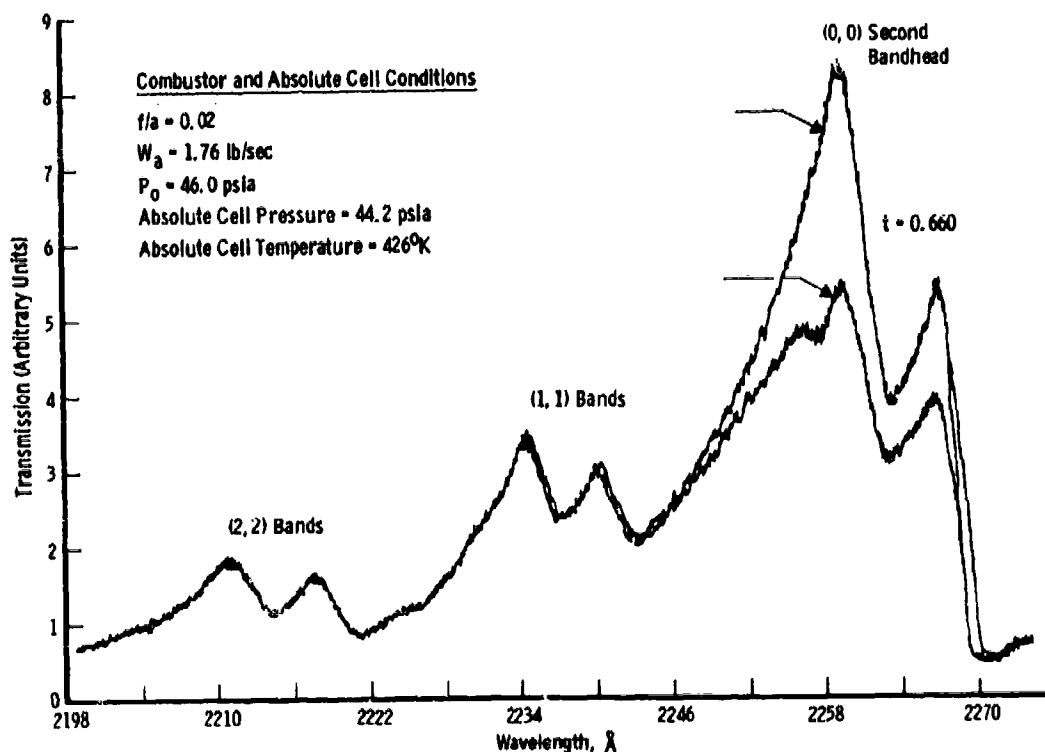
Figure 16. Example spectral scan of the NO (0,0) γ-band transmission taken from sample transfer line absorption cell.
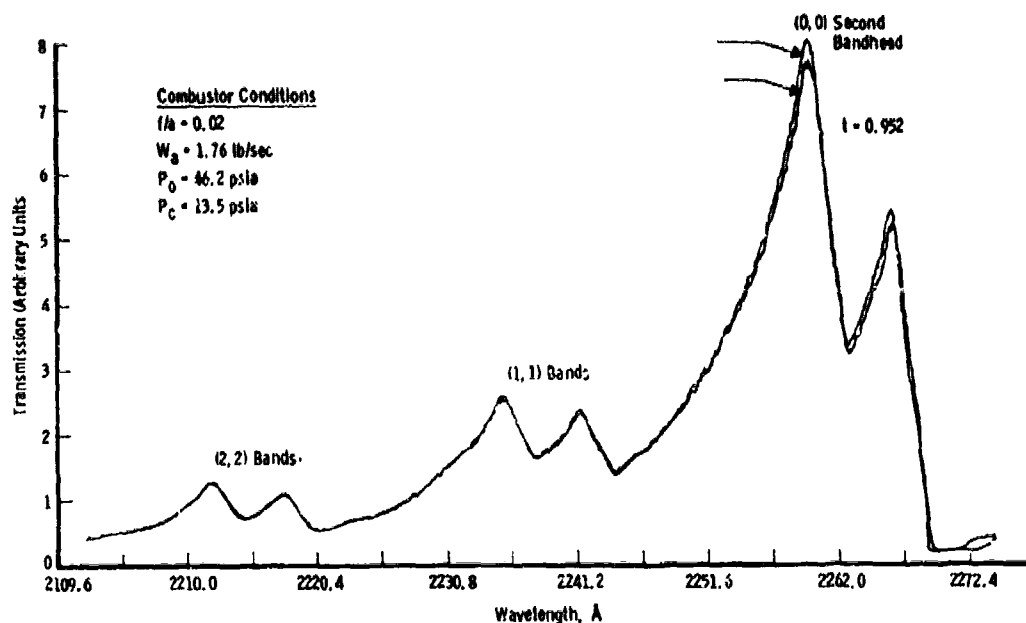
Figure 17. Example spectral scan of the NO (0,0) γ-band transmission
taken from combustor nozzle exit.

Table 4. Concentration of NO in Absorption Cell Located in
Sample Gas Transfer Line

Fuel to Air Ratio	Inlet Air Temperature, °K	Air Mass Flow, lb/sec	Absorption Cell Temperature, °K	Absorption Cell Pressure, psia	Path Length, cm	Broadening Parameter, a'	One Minus Transmission	Absorption Measurement NO Concentration, ppmv	Probe Measurement NO Concentration ppmv
0.012	608	2.58	426	35.00	62.5	7.09	0.246	60	44
0.012	609	2.62	426	35.00	62.5	7.09	0.246	60	45
0.020	568	1.79	426	21.13	62.5	4.28	0.350	130	109
0.020	569	1.76	426	44.22	62.5	8.96	0.340	100	95
0.028	572	1.81	426	18.65	62.5	3.78	0.475	230	201
0.030	608	1.79	426	18.65	62.5	3.78	0.494	220	202
0.030	600	1.70	426	21.13	62.5	4.28	0.422	195	167
0.030	572	1.80	426	35.00	62.5	7.09	0.453	250	191
0.031	571	1.78	426	15.90	62.5	3.22	0.455	240	198
0.037	602	1.62	426	21.13	62.5	4.28	0.416	195	202
0.039	611	1.82	426	15.00	62.5	3.04	0.531	275	233
0.039	572	1.79	426	18.65	62.5	3.78	0.508	230	213
0.040	602	1.70	426	24.66	62.5	5.00	0.565	240	216
0.040	572	1.78	426	28.60	62.5	5.80	0.541	250	174
0.049	603	1.70	426	21.13	62.5	4.28	0.524	230	...
0.050	573	1.78	426	21.13	62.5	4.28	0.609	260	264

31

Table 5. Concentration of NO in Combustor Exhaust 0.5 in. Downstream of Nozzle Exit

Fuel to Air Ratio	Inlet Air Temperature, °K	Air Mass Flow, lb/sec	Combustor Total Pressure, psia	Average Static Pressure, psia	Average Static Temperature, °K	Broadening Parameter °K	Path Length, cm	One Minus Transmission	In Situ Measurement NO Concentration, ppmv	Average Probe Measurement NO Concentration, ppmv
0.010	598	2.500	56.4	20.2	789	2.21	6.0	0.021	175	30
0.019	566	1.767	45.7	15.0	1,031	1.26	6.0	0.060	630	
0.020	598	1.760	44.2	15.0	1,022	1.27	6.0	0.048*	605	102
0.021	606	2.540	66.8	22.0	1,172	1.62	6.0	0.060*	625	
0.021	600	2.008	51.9	17.1	1,130	1.31	6.0	0.057*	600	
0.030	600	1.928	54.4	17.1	1,332	1.11	6.0	0.069	860	190
0.030	591	1.728	49.6	16.2	1,376	1.02	6.0	0.069	860	
0.035	601	2.006	59.8	18.2	1,471	1.07	6.0	0.067	910	
0.039	602	1.771	53.7	17.7	1,548	0.59	6.0	0.070	1,080	
0.039	598	1.769	34.0	17.5	1,546	0.98	6.0	0.071*	1,085	
0.040	604	1.714	52.1	16.7	1,550	0.93	6.0	0.080	1,220	215
0.042	601	2.013	62.2	18.6	1,601	1.00	6.0	0.080*	1,230	
0.049	604	1.700	55.0	16.6	1,702	0.84	6.0	0.060	1,575	
0.051	605	1.778	57.0	18.1	1,724	0.91	6.0	0.090*	1,600	264

*Absorption Cell No. 1
(All Others - Cell No. 2)

<u>Sym</u>

- ▫ Probe Sample Data - Commercial Chemiluminescent Analyzer
- △ Sample Transfer Line Absorption Data
- ○ In Situ Absorption Data - Combustor Exit
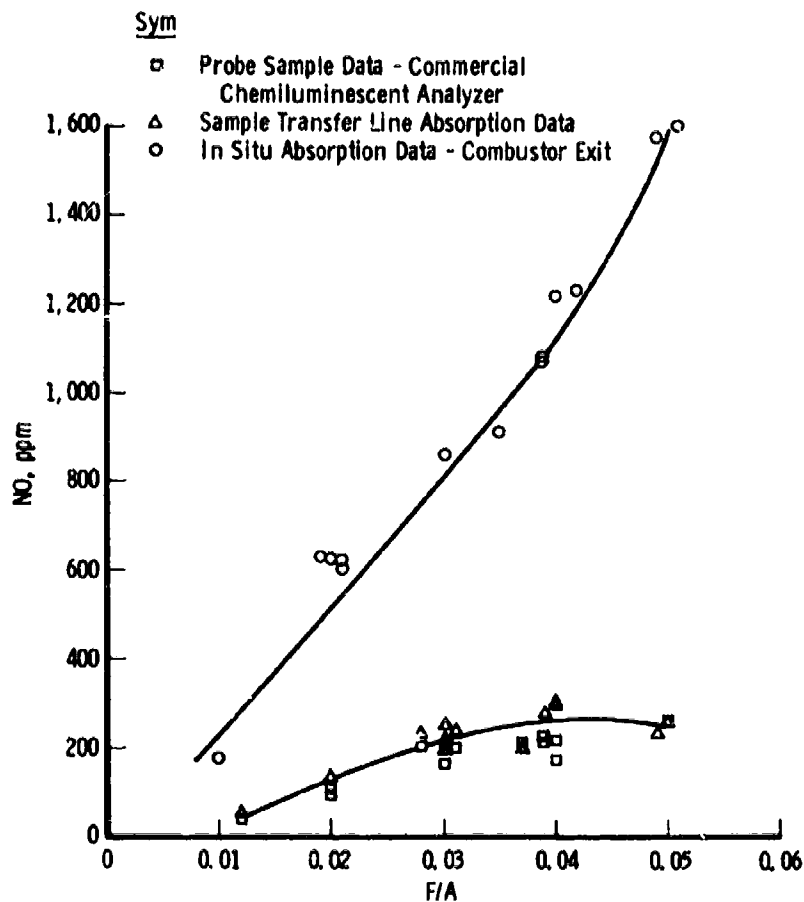
Figure 18. NO concentration as a function of the fuel-to-air ratio for turbine engine combustor exhaust obtained by various means.

4.3 DISCUSSION

4.3.1 Uncertainty

It is not possible to accurately estimate the uncertainty in the in situ optical measurements of NO concentration in the combustor exhaust stream. Factors which influence the uncertainty are the measurement of the second bandhead transmissivity (±0.005), the determination of the static pressure and temperature, the effect of gradients in pressure and temperature on the calculations, and accuracy of the parameters used in the transmission calculation. Of all these effects, the measurement of transmissivity appears to introduce the most error since, for the combustor installation used in this study, values of transmissivity were greater than about 0.9. Thus the inability to measure within about ±0.005 represents an error of about ±5 percent, which represents an uncertainty in concentration for the conditions corresponding to Fig. 14 of ±15 percent. The uncertainty in knowledge of static pressure and temperature (Fig. 12) does not result in an appreciable uncertainty in the concentration. The most important effect of parameter uncertainties is in the value of the broadening parameter, a'. The limits placed on the value of a' (Ref. 12) by the uncertainty in the constant of Eq. (5) (1270 ±200) produces an uncertainty of about ±10 percent in the values of the concentration. Thus, the maximum uncertainty is believed to be no greater than about ±20 percent.

The uncertainty in the concentration measurements from the absorption cells located within the sample transfer lines depends mainly on the uncertainty caused by the uncertainty in a'. Here the effect on the concentration measurement of the uncertainty in measurement of the second bandhead transmissivity (again about ±0.005) is small since values of transmissivity are less than about 0.75. An error of 0.005 in transmissivity for the condition of Fig. 10 gives an uncertainty in concentration of less than ±2 percent. In the absorption cell the temperature and pressure are measured quantities, and there are no gradients along the optical path. Thus the major uncertainty is in the effect of uncertainties in a', which for typical conditions in the absorption cells represents an uncertainty in concentration of about ±5 percent.

4.3.2 Impact of Results

The results shown in Tables 4 and 5 and Fig. 18 make it evident that NO molecules are being converted or destroyed between the inlet to the sample probe and the first absorption cell. Determination of the mechanism by which the NO is converted to some other species is beyond the scope of this study.

The impact of these findings on standardization of measurement techniques for NO emissions is evident. The determination of the actions necessary to circumvent the

33

problem is not so evident. One solution would be to develop the optical technique to the point that it could be used routinely in the field. Such an approach would require a great deal of effort in hardware and software development. A second approach might be to determine the cause of the NO loss and to design sampling probes that would not suffer the loss. The second approach appears to be a complex one requiring extensive research. The impact of the much larger NO concentrations found by the in situ measurements on such programs as the Climatic Impact Assessment Program (CIAP, Ref. 16) and the development of low emission engines required to meet standards of the Environmental Protection Agency (EPA) are also evident. The findings reported here indicate that the extent of the combustor development necessary to meet the standards of either of these programs may be much greater than originally believed.

5.0 SUMMARY

Measurements of the NO concentration in the exhaust of a turbine engine combustor were made over a range of fuel-to-air ratios from 0.01 to 0.05 at an inlet air temperature of about 600°F and total pressure of about 3 to 4 atm by both conventional gas sampling probes and optical absorption methods. The absorption measurements were made both directly through the combustor exhaust stream and through the absorption cells located within the gas sample transfer line. The results of the measurements are as follows:

1. The measured NO concentrations increase with the fuel-to-air ratio regardless of which measurement technique is used.

2. The NO concentration measured using the conventional gas analyzer was very nearly the same (within about 20 percent) as that measured using the optical method in the absorption cells located within the gas sample transfer line, ranging from about 30 ppmv at f/a = 0.1 to 264 ppmv at f/a = 0.05.

3. The NO concentration measured using the optical absorption method through the combustor exhaust stream ranged from about 175 ppmv at f/a = 0.01 to 1,600 ppmv at f/a = 0.05.

4. The NO concentration measured using the optical absorption method through the combustor exhaust stream was larger than that measured by the conventional gas analyzer by a factor of about 3.5 to 6, depending on the f/a ratio.

REFERENCES

1. SAE Aerospace Recommended Practice 1256, "Procedure for the Continuous Sampling and Measurement of Gaseous Emissions from Aircraft Turbine Engines." Society of Automotive Engineers, New York, October 1, 1971.

2. Gearhart, J. W. and Benek, J. A. "Measurement of Pollutant Emissions from an Afterburning Turbojet Engine at Ground Level: I. Particulate Emissions." AEDC-TR-72-64 (AD744048), June 1972.

3. Lazalier. G. R. and Gearhart, J. W "Measurement of Pollutant Emissions from an Afterburning Turbojet Engine at Ground Level: II. Gaseous Emissions." AEDC-TR-72-70 (AD747773), August 1972.

4. Davidson, D. L. and Domal, A. F. "Emission Measurements of a J93 Turbojet Engine." AEDC-TR-73-132 (AD766648), September 1973.

5. German, R. C., High, M. D. and Robinson, C. E. "Measurement of Exhaust Emissions from a J85-GE-5B Engine at Simulated High-Altitude, Supersonic Free-Stream Flight Conditions." AEDC-TR-73-103 (AD764717), July 1973.

6. Davis, M. G., McGregor, W. K. and Mason, A. A. "OH Chemiluminescent Radiation from Lean Hydrogen-Oxgyen Flames." The Journal of Chemical Physics, Vol. 61, No. 4, 15 August 1974, pp. 1352-1356.

7. McGregor, W. K., Few, J. D., and Litton, C. D. "Resonance Line Absorption Method for Determination of Nitric Oxide Concentration." AEDC-TR-73-182 (AD771642), December 1973.

8. McGregor, W. K., Seiber, B. L., and Few, J. D. "Concentration of OH and NO in YJ93-GE-3 Engine Exhaust Measured In Situ by Narrow-Line UV Absorption." Proceedings of the 2nd Conference on the Climatic Impact Assessment Program, Cambridge, Massachusetts, November 1972.

9. Thompson, J. W., Jr. and Abernethy, R. B. et al. "Handbook: Uncertainty in Gas Turbine Measurements." AEDC-TR-73-5 (AD755356), February 1973.

10. Williamson, R. C. and Stanforth, C. M. "The Evaluation of Factors Which Influence Accuracy Based Upon Experience in Measurement of Aircraft Exhaust Emissions." Presented at the Third Joint Environmental Instrumentation and Control Symposium. New York, October 1974.

11. Davis, M. G., McGregor, W. K. and Few, J. D. "Spectral Simulation of Resonance Band Transmission Profiles for Species Concentration Measurements: NO γ-Bands as an Example." AEDC-TR-74-124 (ADA004105), January 1975.

12. Davis, M. G., McGregor, W. K., Few, J. D., and Glassman, H. N. "The Transmission of Doppler Broadened Resonance Radiation Through Absorbing Media with Combined Doppler and Pressure Broadening (NO γ-Bands as an Example)." AEDC-TR-76-12 (ADA021061), February 1976.

13. "User Manual - Description of a Digital Computer Program for Nozzle and Plume Analysis by Method of Characteristics." TM-54/20/-108, Lockheed Missile and Space Company, Sunnyvale, California, December 1966.

14. Osgerby, I. T. and Rhodes, R. P. "An Efficient Numerical Method for the Calculation of Chemical Equilibrium in the H/C/O/N/A System." AEDC-TR-71-256 (AD741825), April 1972.

15. Harsha, P. T. "Free Turbulent Mixing. A Critical Evaluation of Theory and Experiment." AEDC-TR-71-36 (AD718956), February 1971.

16. Grobecker, A. J., Coroniti, S. C. and Cannon, R. H., Jr. "The Effects of Stratospheric Pollution by Aircraft." DOT-TST-75-50, December 1974.

APPENDIX A
PROPERTIES OF THE RESONANCE SOURCE OF NO γ-BAND RADIATION

The spectral intensity distribution of the lines within vibration-rotation bands of diatomic molecules emitted from a gas discharge tube do not follow any predictable pattern. This result is caused by the nature of the excitation of the molecules via high energy electron collisions. Therefore, to be useful in a model of the transmission of resonance radiation from a gas discharge source through an absorbing medium, the distribution of the intensities of the lines must be determined experimentally.

A sketch of the discharge tube used to produce a resonance source of NO γ-band radiation is shown in Fig. I-1. The discharge is viewed end-on through the capilliary tube. The mixture of gas found experimentally to be most useful for producing the NO γ-bands was a 12:3:1 mixture by volume of $A:N_2:O_2$. The gas flows through the tube at about 36 liters/hr at a pressure of about 6 torr at the inlet of the tube and emerges at a pressure of about 4 torr. Cooling water flow is supplied at a rate of about 500 gm/hr.
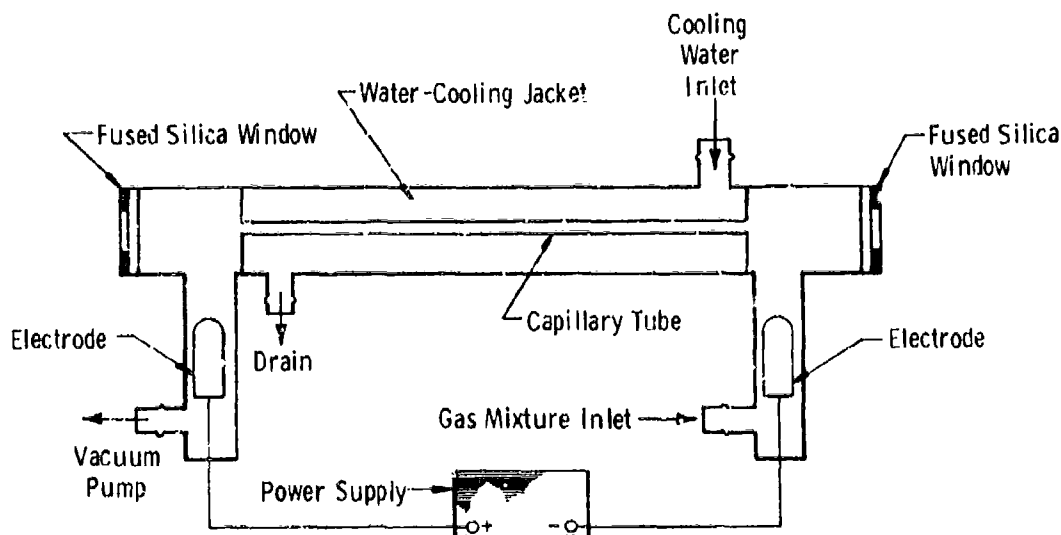
Figure A-1. Diagram of discharge tube used to produce narrow-line radiation.

The spectrum at approximately 0.03-Å resolution of the (0,0) γ-band is shown in Fig. A-2. The spectrum was obtained by use of a 1-m grating instrument operating in second order. Many nonoverlapping lines of the (0,0) γ-band of NO are isolated in Fig. A-2, and these can be used to determine an empirical intensity distribution function to predict intensities of lines that cannot be isolated because of overlapping or lack of resolution.

Figure A-2. Discharge tube spectrum showing (0,0) γ-band of NO
at 0.03-Å resolution.

The determination of the distribution function is discussed more completely in Ref. 11 but is given here because it plays such a great part in the transmission model. Fig. A-3 shows the intensity, $I_{\nu_j}^{o}$, distribution of the 0,0 γ-band as a function of the energy, $F_{J'}$, of the $A^2\Sigma$ state of NO, the upper state for the γ-band system. The intensity of each line is divided by the rotational strength factor, $S_{J'J''}$, for convenience in the calculations.

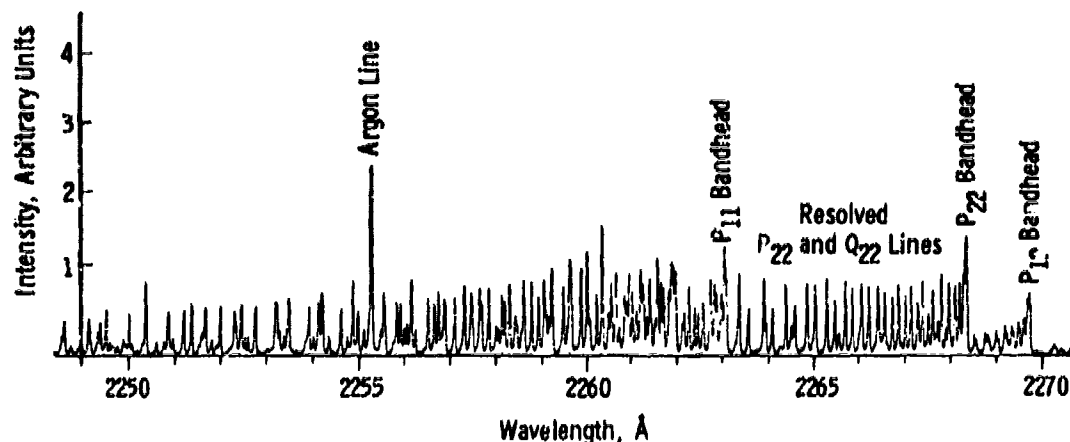Another property of the radiation source which must be supplied to the resonance transmission model for the NO γ-bands is the temperature of the gas within the capilliary tube, T_s. The gas discharge tube is operated at low pressure, and the gas flows continuously through it. The capilliary tube is surrounded by a water-cooling passage. Furthermore, the cathode is placed on the downstream side of the capilliary (see Fig. A-1) so that most of the gas heating by the electrical discharge occurs after the gas has passed through the capilliary. Very little heating occurs in the positive column the capilliary in this case, of a discharge tube. It is not possible to measure T_s directly. Thermocouple measurements in the gas line for a typical case showed a rise from 21 to 23°C at the extremities of the discharge tube. Thermocouple readings in the cooling water flow (about 500 gm/hr) gave less than 1°C rise. Heat-transfer analysis of the capilliary region predicted a maximum temperature rise of the gas of about 5°C for the 1°C water temperature rise; therefore, it was concluded that the temperature in the capilliary was about 300°K.

Since the estimate of the source gas temperature made in this way is inexact, a study of the effect of any error in T_s on the simulated transmission spectra was made. It
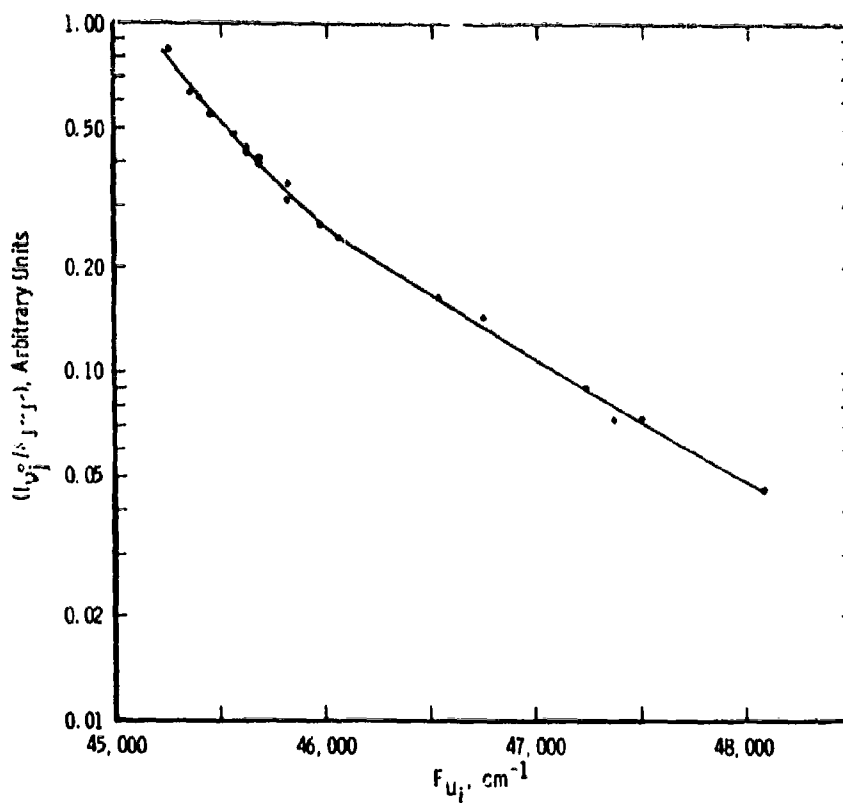
Figure A-3. Population distribution of excited rotational states of
$A_2 \psi$ level of NO in resonance lamp containing a
12:3:1 mixture by volume of $Ar:N_2:O_2$ operated
at a 6-ton pressure with 2,800v DC applied.

was found that changing T_s from 300 to 320°K (maximum temperature imaginable), for an atmospheric pressure absorbing media at 422°K, would result in a change in the transmissivity of the 0,0 γ-band at the second bandhead of less than 0.5 percent of the transmissivity, as shown in the table below for an absorber temperature of 422°K and a pressure of 1 atm.

NO Density	Computed Second Bandhead Transmissivity, percent	
	$T_s = 300°K$	$T_s = 320°K$
1.36×10^{14}	94.8	94.8
3.31×10^{14}	88.1	88.0
1.33×10^{15}	61.7	61.5
2.75×10^{15}	39.1	33.9

Thus the transmission is not a sensitive function of the source temperature so long as the temperature of the gas is a few hundred degrees Kelvin higher than that of the source. The transmission model was exercised at $T_s = 320°K$ for the computations in this study.

NOMENCLATURE

a'	Line-broadening parameter
B_0	Rotational constant for the ground state, cm^{-1}
c	Velocity of light, 3×10^{10} cm/sec
e	Electronic charge, 4.80×10^{-10} esu
F(J")	Rotational energy of the J"th rotational state, cm^{-1}
$f_{J'J"}$	Oscillator strength for the transition from the upper state J' to the lower state J"
$f_{v'v"}$	Band oscillator strength for the v' - v" vibrational transition
h	Planck's constant, 6.625×10^{-27} erg sec
I_{ν_j}	Intensity of source spectral line at center wavenumber, ν_j, intensity units
$I\beta_j$	Intensity of source spectral line at wavenumber, ν_j, intensity units
J'	Rotational quantum number for the upper state
J"	Rotational quantum number for lower state
k_{ν_j}, k_{ν_i}	Absorption coefficient for spectral line at wavenumber, ν_j or ν_i, cm^{-1}
$k\beta_j, k\beta_i$	Absorption coefficient at center wavenumber ν_j or ν_i, cm^{-1}
ℓ	Absorption path length, cm
M_a, M_s	Mass of molecules in absorber and light source, gm
m	Electron mass, 9.11×10^{-28} gm
$N_{J"}$	Number density of molecules in the lower state, J", cm^{-3}
N_0	Total number density of molecules, cm^{-3}

n	Integer used to set limits of integration
P_c	Cell pressure
P_o	Plenum pressure
p	Static pressure, atm
S	Total electron spin quantum number
$S_{J''J'}$	Rotational strength, or Honl-London factor, for the $v'J' - v''J''$ vibrational-rotational transition
T_a	Temperature of absorber gas, °K
T_s	Temperature in light source, °K
$t_{\Delta\nu}$	Transmissivity over the frequency interval $\Delta\nu$; ratio of incident to transmitted intensity
W_a	Inlet air weight flow rate
y	Dummy variable of integration
$(\Delta_a\nu_i)_D$	Doppler width at half maximum absorption coefficient, k_{ν_i}, of the absorption line, i, cm⁻¹
$(\Delta_a\nu_i)_L$	Lorentz half width at half maximum absorption coefficient due to collision broadening of the absorption line, i, cm⁻¹
$(\Delta_s\nu_j)_D$	Doppler width at half maximum intensity, $I^o_{\nu_j}$, of the emission line, cm⁻¹
$\Delta\nu$	Wavenumber increments, cm⁻¹
K	Boltzmann's constant, 0.6952 cm⁻¹ °K⁻¹
ν	Wavenumber, cm⁻¹
ν_i, ν_j	Center wavenumber of the ith or j^{th} spectral line, cm⁻¹
$\nu_{J'J''}$	Wavenumber of the line corresponding to the transition $v'J' - v''J''$, cm⁻¹
$\nu_{v'v''}$	Wavenumber at the bandhead of the (v', v'') band, cm⁻¹
π	Pi, 3.14159
ω_i	Doppler frequency function

41

SUPPLEMENTARY

INFORMATION

ERRATA

AEDC-TR-76-180, January 1977
(UNCLASSIFIED REPORT)

EVALUATION OF PROBE SAMPLING VERSUS OPTICAL IN SITU MEASUREMENTS OF NITRIC OXIDE CONCENTRATIONS IN A JET ENGINE COMBUSTOR EXHAUST

J. D. Few, R. J. Bryson, and W. K. McGregor, ARO, Inc.

Arnold Engineering Development Center
Air Force Systems Command
Arnold Air Force Station, Tennessee

Tables 4 and 5 and Figs. 16 and 17, pp. 30 to 32 in subject report, have been revised and are reproduced here.

Table 4. Concentration of NO in Absorption Cell Located in Sample Gas Transfer Line

Fuel to Air Ratio	Inlet Air Temperature, °K	Air Mass Flow, lb/sec	Absorption Cell Temperature, °K	Absorption Cell Pressure, psia	Path Length, cm	Broadening Parameter, a'	One Minus Transmission	Absorption Measurement NO Concentration, ppmv	Probe Measurement NO Concentration, ppmv
0.012	608	2.58	426	35.00	62.5	7.09	0.246	60	44
0.012	609	2.62	426	35.00	62.5	7.09	0.246	60	45
0.020	568	1.79	426	21.13	62.5	4.28	0.350*	130	109
0.020	569	1.76	426	44.22	62.5	8.96	0.340*	100	95
0.028	572	1.81	426	18.65	62.5	3.78	0.475*	230	201
0.030	608	1.79	426	18.65	62.5	3.78	0.494	220	202
0.030	600	1.70	426	21.13	62.5	4.28	0.422	195	167
0.030	572	1.80	426	35.00	62.5	7.09	0.453*	250	191
0.031	571	1.78	426	15.90	62.5	3.22	0.455	240	198
0.037	602	1.62	426	21.13	62.5	4.28	0.416	195	202
0.039	611	1.82	426	15.00	62.5	3.04	0.531	275	233
0.039	572	1.79	426	18.65	62.5	3.78	0.508	230	213
0.040	602	1.70	426	24.66	62.5	5.00	0.565	240	216
0.040	572	1.78	426	28.60	62.5	5.80	0.541	250	174
0.049	603	1.70	426	21.13	62.5	4.28	0.524*	230	---
0.050	573	1.78	426	21.13	62.5	4.28	0.609	260	264

*Absorption Cell No. 1
(All Others - Cell No. 2)

Table 5. Concentration of NO in Combustor Exhaust 0.5 in. Downstream of Nozzle Exit

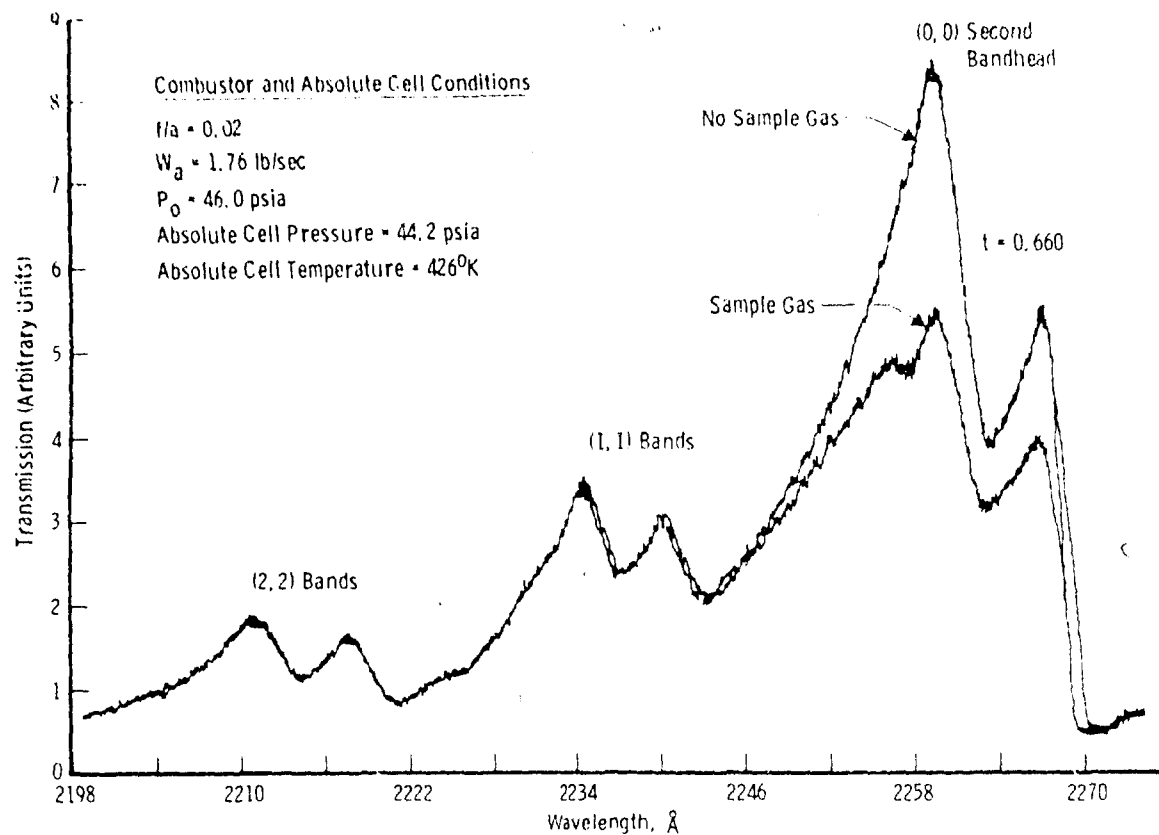| Fuel to Air Ratio	Inlet Air Temperature, °K	Air Mass Flow, lb/sec	Combustor Total Pressure, psia	Average Static Pressure, psia	Average Static Temperature, °K	Broadening Parameter, °K	Path Length, cm	One Minus Transmission	In Situ Measurement NO Concentration, ppmv	Average Probe Measurement NO Concentration, ppmv
0.010	598	2,500	56.4	20.2	789	2.21	60	0.021	175	30
0.010	566	1,767	45.7	15.0	1,031	1.26	60	0.060	630	
0.020	598	1,760	46.2	15.0	1,022	1.27	60	0.048	605	102
0.021	606	2,540	66.8	22.0	1,172	1.62	60	0.060	625	
0.021	600	2,008	51.9	17.1	1,130	1.31	60	0.057	600	
0.030	600	1,928	54.4	17.1	1,332	1.11	60	0.069	860	190
0.030	591	1,728	49.6	16.2	1,376	1.02	60	0.069	860	
0.035	601	2,008	59.8	18.2	1,471	1.07	60	0.067	910	
0.039	602	1,774	53.7	17.7	1,548	0.99	60	0.070	1,080	
0.039	598	1,769	54.0	17.5	1,546	0.98	60	0.071	1,085	
0.040	604	1,714	52.1	16.7	1,550	0.93	60	0.080	1,220	215
0.042	601	2,013	62.2	18.6	1,601	1.00	60	0.080	1,230	
0.049	604	1,700	55.0	16.6	1,702	0.84	60	0.080	1,575	
0.051	605	1,778	57.0	18.1	1,774	0.91	60	0.090	1,600	264

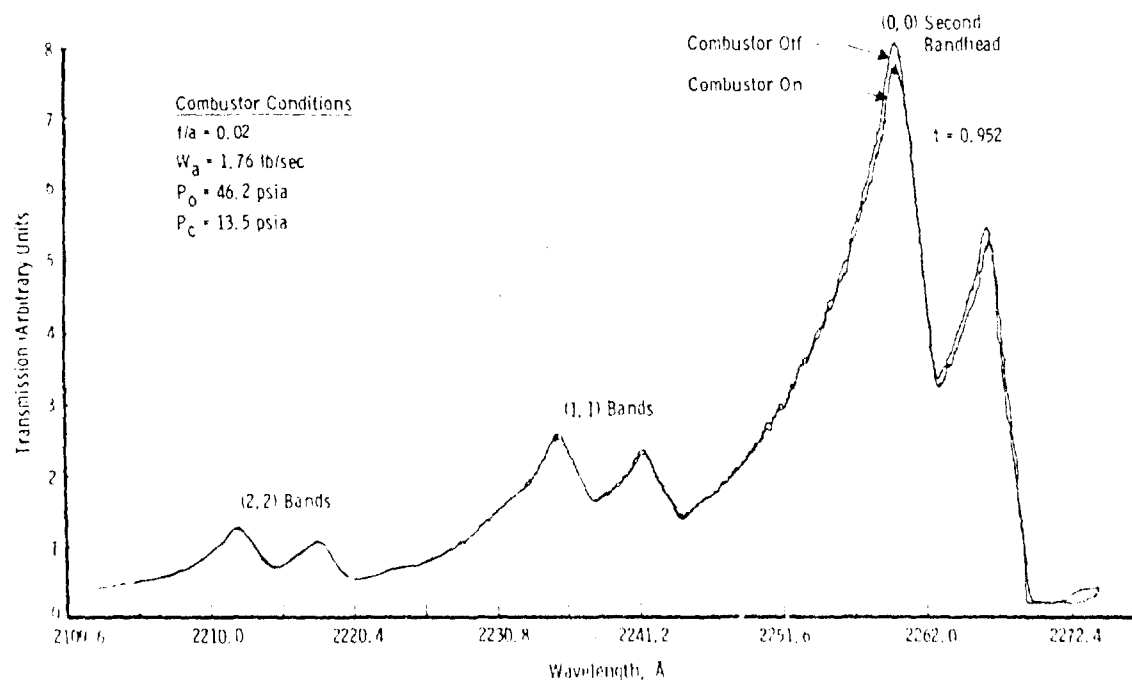Figure 16. Example spectral scan of the NO (0,0) γ-band transmission taken from sample transfer line absorption cell.

Figure 17. Example spectral scan of the NO (0,0) γ-band transmission taken from combustor nozzle exit.

SUPPLEMENTARY

INFORMATION

ERRATA

AEDC-TR-76-180, January 1977
(UNCLASSIFIED REPORT)

EVALUATION OF PROBE SAMPLING VERSUS OPTICAL
IN SITU MEASUREMENTS OF NITRIC OXIDE
CONCENTRATIONS IN A JET ENGINE COMBUSTOR EXHAUST

J. D. Few, R. J. Bryson, and W. K. McGregor
ARO, Inc.

Arnold Engineering Development Center
Air Force Systems Command
Arnold Air Force Station, Tennessee 37389

Errors have been found in the theoretical model as presented in
Eqs. (10) through (13) on page 20. Consequently, the data presented in
Figs. 9, 10, 13, 14, and 18 and in Tables 4 and 5, obtained using the
model, must be considered suspect.

An AEDC Technical Report containing the correct model and corrected
data will be issued.